Article

Enterococci enhance *Clostridioides difficile* pathogenesis

https://doi.org/10.1038/s41586-022-05438-x

Received: 17 May 2021

Accepted: 11 October 2022

Published online: 16 November 2022

Check for updates

Alexander B. Smith[1], Matthew L. Jenior[2], Orlaith Keenan[1], Jessica L. Hart[1], Jonathan Specker[3], Arwa Abbas[1], Paula C. Rangel[1], Chao Di[4], Jamal Green[5], Katelyn A. Bustin[6], Jennifer A. Gaddy[7,8], Maribeth R. Nicholson[9], Clare Laut[7], Brendan J. Kelly[10], Megan L. Matthews[6], Daniel R. Evans[11], Daria Van Tyne[11], Emma E. Furth[12], Jason A. Papin[2], Frederic D. Bushman[12], Jessi Erlichman[13], Robert N. Baldassano[5,13], Michael A. Silverman[5,14], Gary M. Dunny[15], Boone M. Prentice[3], Eric P. Skaar[7] & Joseph P. Zackular[1,16,17] ✉

Enteric pathogens are exposed to a dynamic polymicrobial environment in the gastrointestinal tract[1]. This microbial community has been shown to be important during infection, but there are few examples illustrating how microbial interactions can influence the virulence of invading pathogens[2]. Here we show that expansion of a group of antibiotic-resistant, opportunistic pathogens in the gut—the enterococci—enhances the fitness and pathogenesis of *Clostridioides difficile*. Through a parallel process of nutrient restriction and cross-feeding, enterococci shape the metabolic environment in the gut and reprogramme *C. difficile* metabolism. Enterococci provide fermentable amino acids, including leucine and ornithine, which increase *C. difficile* fitness in the antibiotic-perturbed gut. Parallel depletion of arginine by enterococci through arginine catabolism provides a metabolic cue for *C. difficile* that facilitates increased virulence. We find evidence of microbial interaction between these two pathogenic organisms in multiple mouse models of infection and patients infected with *C. difficile*. These findings provide mechanistic insights into the role of pathogenic microbiota in the susceptibility to and the severity of *C. difficile* infection.

Enteric infections are polymicrobial by nature, as pathogens become exposed to a rich microbial ecosystem and complex metabolic environment during invasion of the gastrointestinal tract. The study of pathogen–microbiota interactions during infection is central to our ability to understand and treat enteric infections. One of the most significant enteric pathogens globally is *Clostridioides difficile*[3], but little is known about how *C. difficile* cooperates with the rich collection of microorganisms in the gastrointestinal tract.

Enterococci are enriched in the *C. difficile*-infected gut and vancomycin-resistant *Enterococcus* (VRE) frequently co-infects patients with *C. difficile*[2,4–10]. However, the effect of *Enterococcus* on susceptibility to *C. difficile* infection (CDI) and clinical outcomes remains unknown. To further define the association between *Enterococcus* and *C. difficile* during infection, we quantified *Enterococcus* burdens in paediatric patients with CDI. Consistent with studies in adults, we found an enrichment of enterococci in the stool of paediatric patients with CDI (Extended Data Fig. 1a) and a positive correlation between enterococcal and *C. difficile* burdens (Spearman $\rho = 0.551$, $n = 19$) (Extended Data Fig. 1b). These data confirm that enterococci are highly abundant in the CDI gut and positively correlate with *C. difficile* burden.

Enterococcal–*C. difficile* interactions

To determine a causal role for enterococci in susceptibility to CDI, we infected mice with *C. difficile* following antibiotic-mediated depletion of endogenous enterococci. Mice given cefoperazone, which does not target enterococci, showed robust *C. difficile* colonization one day after infection (Fig 1a and Extended Data Fig. 1c). However, enterococcal depletion with cefoperazone and vancomycin resulted in a delay of *C. difficile* colonization (Fig 1a and Extended Data Fig. 1c). To test whether this was a direct effect of enterococci, we introduced *Enterococcus faecalis* (strain OG1RF) immediately preceding CDI. Introduction of *E. faecalis* into the enterococcal-depleted gut recovered early *C. difficile* colonization on day one after infection (Fig. 1a). This indicated that enterococci may alter the gastrointestinal environment following antibiotic treatment and support *C. difficile* during early colonization events. To test the reciprocal effect of *C. difficile* on enterococcal fitness

[1]Division of Protective Immunity, Children's Hospital of Philadelphia, Philadelphia, PA, USA. [2]Department of Biomedical Engineering, University of Virginia, Charlottesville, VA, USA. [3]Department of Chemistry, University of Florida, Gainesville, FL, USA. [4]Department of Biomedical and Health Informatics, Children's Hospital of Philadelphia, Philadelphia, PA, USA. [5]Department of Pediatrics, Perelman School of Medicine, University of Pennsylvania, Philadelphia, PA, USA. [6]Department of Chemistry, School of Arts and Sciences, University of Pennsylvania, Philadelphia, PA, USA. [7]Department of Pathology, Microbiology, and Immunology, Vanderbilt University School of Medicine, Nashville, TN, USA. [8]Department of Medicine, Vanderbilt University Medical Center, Nashville, TN, USA. [9]Department of Pediatrics, Vanderbilt University School of Medicine, Nashville, TN, USA. [10]Department of Medicine, Division of Infectious Diseases & Department of Biostatistics, Epidemiology, and Informatics, University of Pennsylvania, Philadelphia, PA, USA. [11]Department of Medicine, Division of Infectious Diseases, University of Pittsburgh, Pittsburgh, PA, USA. [12]Department of Microbiology, Perelman School of Medicine, University of Pennsylvania, Philadelphia, PA, USA. [13]Division of Gastroenterology, Hepatology, and Nutrition, Children's Hospital of Philadelphia, Philadelphia, PA, USA. [14]Division of Pediatric Infectious Diseases, Children's Hospital of Philadelphia, Philadelphia, PA, USA. [15]Department of Microbiology, University of Minnesota Medical School, Minneapolis, MN, USA. [16]Department of Pathology and Laboratory Medicine, Perelman School of Medicine, University of Pennsylvania, Philadelphia, PA, USA. [17]Institute for Immunology, Perelman School of Medicine, University of Pennsylvania, Philadelphia, PA, USA. ✉e-mail: joseph.zackular@pennmedicine.upenn.edu

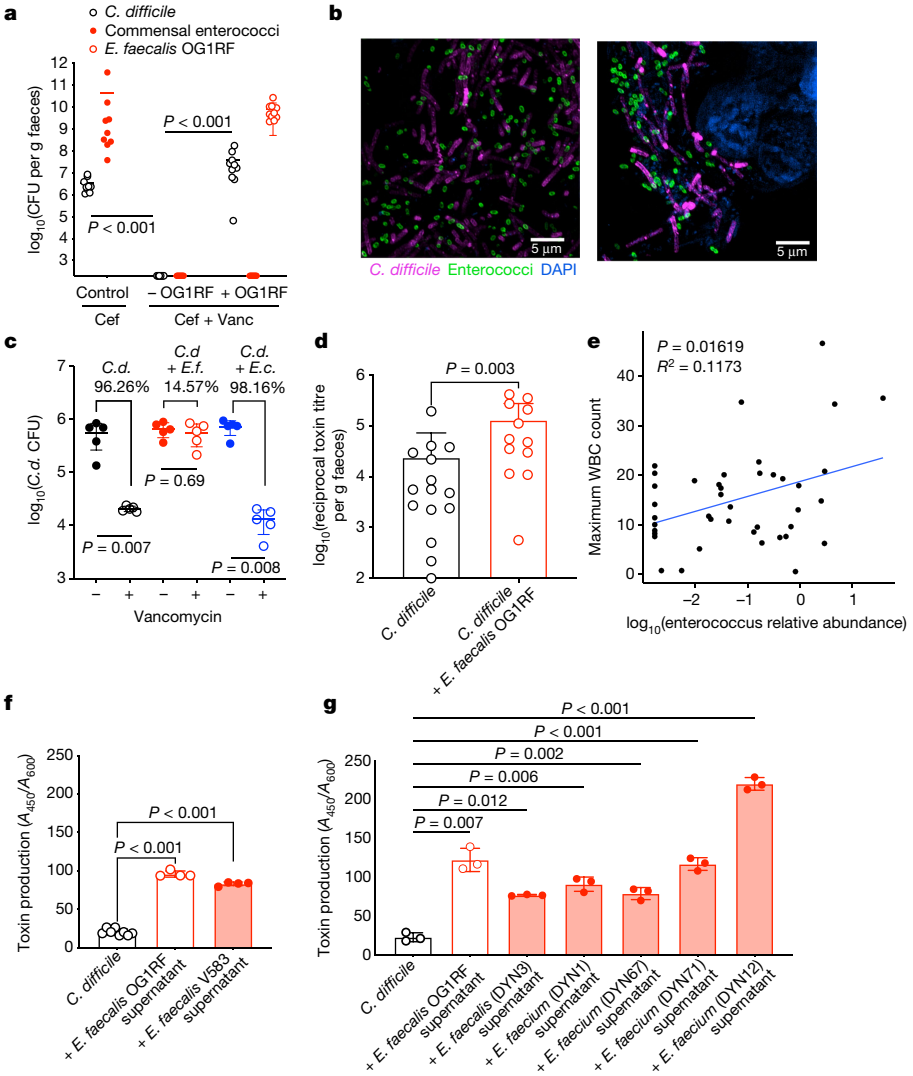

Fig. 1 | Enterococci promote *C. difficile* fitness and pathogenesis. **a**, Bacterial burdens of endogenous enterococci measured on the day of *C. difficile* inoculation. *C. difficile* burdens were measured one day after inoculation to determine success of the initial colonization. Burdens were calculated following treatment with cefoperazone (cef) or cefoperazone plus vancomycin (vanc) with or without *E. faecalis* OG1RF. Data are mean ± s.d., $n = 10$ per group; two-sided Mann–Whitney test for each comparison. CFU, colony-forming units. **b**, FISH image in lumen (left) or associated with the mucosa (right) during mouse infection. **c**, *C. difficile* CD196 (*C.d.*) burden in biofilms of monocultures or co-cultures with *E. faecalis* (*E.f.*) or *E. coli* (*E.c.*). Biofilms treated with vehicle or 5 μg ml^{-1} vancomycin. The percent killing versus untreated is shown above the plot. Data are mean ± s.d., $n = 5$; two-sided Mann–Whitney test. **d**, *C. difficile* toxin titres from mice infected with *C. difficile* or *C. difficile* plus *E. faecalis* OG1RF following treatment with cefoperazone and vancomycin. Data are mean ± s.d., $n = 15$ for *C. difficile* only and $n = 12$ for *C. difficile* + *E. faecalis*; two-sided Mann–Whitney test, $P = 0.003$. **e**, Linear regression relating peripheral WBC count to relative abundance of *Enterococcus* 16S rRNA. $n = 41$; $P = 0.016$. Two-sided Spearman correlation was also performed and showed a positive correlation between WBC count and *Enterococcus* relative abundance (Spearman $\rho = 0.252$, $n = 41$). **f**, *C. difficile* toxin levels measured by enzyme-linked immunosorbent assay (ELISA) following growth with *E. faecalis* supernatants. Data are mean ± s.d., $n = 8$ for *C. difficile* only and $n = 4$ for *E. faecalis* OG1RF and *E. faecalis* V583; one-way Welch ANOVA. **g**, ELISA for *C. difficile* toxin following the introduction of cell-free supernatants from enterococci isolated from paediatric patients with inflammatory bowel disease (IBD) and CDI. Patient IDs begin with DYN. Data are mean ± s.d., $n = 3$ per group; one-way Welch ANOVA.

in the gut, we infected mice with *C. difficile* deficient in toxin production (*tcdA*$^-$*tcdB*$^-$). Enterococci grow out in the antibiotic-treated gut independent of toxin; however, burdens were significantly increased in the presence of *C. difficile* toxin (Extended Data Fig. 1d). These data are consistent with previous studies that demonstrate the ability of enterococci to bloom following antibiotic perturbation[11,12] and further demonstrate that *C. difficile* toxin-mediated damage provides an added fitness advantage.

To test whether enterococci interact with *C. difficile* during infection, we first performed fluorescent in situ hybridization (FISH) during CDI in mice. Enterococci co-localize with *C. difficile* in the lumen (Fig. 1b, left) and in biofilm-like aggregates on the host epithelium (Fig. 1b, right). To examine the potential role of dual-species biofilms, we performed biofilm assays in vitro. *C. difficile* readily forms biofilms with *E. faecalis* and this markedly enhances *C. difficile* survival during vancomycin treatment (Fig. 1c). This phenomenon was not observed in dual-species biofilms with *Escherichia coli*, another member of the microbiota (Fig. 1c). Notably, transposon mutants in genes associated with *E. faecalis* biofilm structure[13,14] (*fsrB*::Tn; OG1RF_11528, *prsA*::Tn; OG1RF_10423) did not provide significant protection for *C. difficile* in the presence of vancomycin (Extended Data Fig. 2a,b). This demonstrates that *E. faecalis* biofilm structure is important for enhancing *C. difficile* survival following antibiotic exposure and suggests that dual-species biofilms may promote persistence during infection.

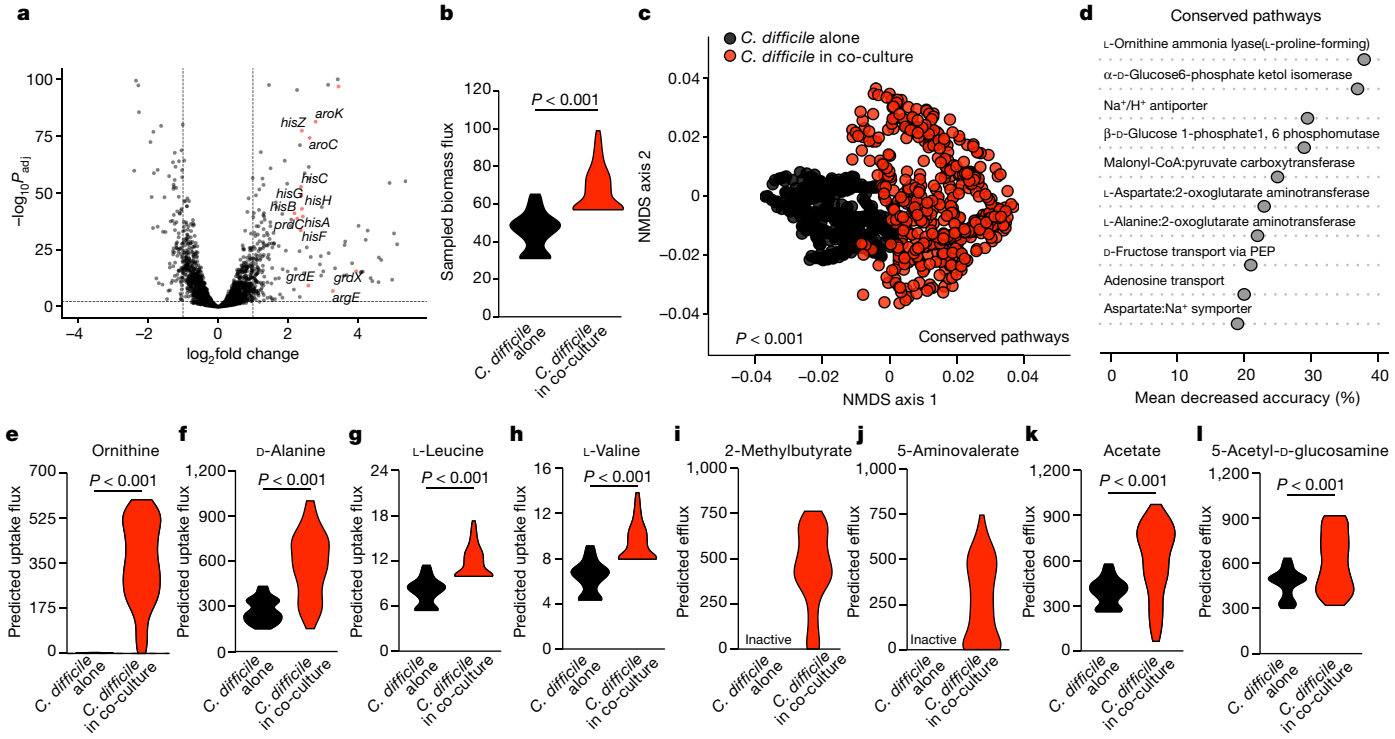

Fig. 2 | Context-specific genome-scale metabolic network reconstruction analysis of *C. difficile* CD196 reveals substantial metabolic shifts when in co-culture with *Enterococcus*. a, Volcano plot showing RNA-sequencing analysis of *C. difficile* transcripts that are altered following co-culture with *E. faecalis*. Two-sided Wald test with Benjamini–Hochberg multiple comparisons correction. Red points denote genes associated with amino acid metabolism. **b**, Sampled metabolic flux states with biomass synthesis as the objective function in each context-specific model. Two-sided Wilcoxon rank-sum test. **c**, Non-metric multidimensional scaling (NMDS) of Bray–Curtis dissimilarities for flux samples of all shared reactions across both experimental contexts. One-way permutational multivariate ANOVA, $P = 0.001$. **d**, Area Under the Curve–Random Forest supervised machine learning results highlighting reactions that differentiate flux distributions during *C. difficile* growth and *C. difficile* growth in the context of *E. faecalis* ($k = 10$; out-of-bag score (OOB) = 0%). **e**–**h**, Difference in simulated uptake of L-ornithine (**e**), D-alanine (**f**), L-leucine (**g**) or L-valine (**h**) across context-specific models. **i**–**l**, Difference in 2-methylbutyrate (**i**), 5-aminovalerate (**j**), acetate (**k**) and *N*-acetyl-D-glucosamine (**l**) efflux across context-specific models. Significance determined by two-sided Wilcoxon rank-sum test.

Biofilms provide ideal conditions for horizontal gene transfer between bacterial species[15]. We postulated that these two organisms may share mobile genetic elements (MGEs) in the gut. Analysis of genomes from *C. difficile* and VRE (*E. faecium* and *E. faecalis*) clinical isolates from co-colonized patients resulted in the detection of six sequence clusters predicted to encode MGEs. The largest gene cluster encoded a Tn916-like tetracycline resistance-carrying transposon[16] (Extended Data Fig. 2c). Surprisingly, we also observed a cluster encoding a transposon carrying a predicted collagen-binding surface adhesin that resembled the CD0386 adhesin, a known *C. difficile* surface protein and substrate of sortase B[17] (Extended Data Fig. 2c). When expressed in *E. faecalis* OG1RF, CD0386 enhanced binding to collagen-coated plates, suggesting that horizontal transfer of genes from *C. difficile* to enterococci can support the fitness of this opportunistic pathogen in the gut (Extended Data Fig. 2d). These data provide evidence of robust MGE transfer between *C. difficile* and VRE during infection.

Enterococci enhance pathogenesis

To examine the effect of enterococci on *C. difficile* pathogenesis, we quantified *C. difficile* toxin titres from the faeces of mice pre-inoculated with *E. faecalis* OG1RF. Mice co-infected with *E. faecalis* showed significantly higher titres of toxin in faeces compared with those infected with *C. difficile* only (Fig. 1e). To examine the clinical relevance of these findings, we evaluated the relationship between *Enterococcus* relative abundance based on 16S rRNA gene sequencing and maximum peripheral white blood cell (WBC) count, a measure of systemic inflammation, in an adult cohort of CDI. *Enterococcus* was positively associated with inflammation based on a linear regression model, with serum WBCs increasing by 3,030 cells per ml for each log increase in *Enterococcus* abundance (s.e.m. 1,200 cells per ml; $P = 0.017$) (Fig. 1e). Spearman correlation analysis further showed a positive correlation between the number of WBCs and *Enterococcus* (Spearman $\rho = 0.252$, $n = 33$). On the basis of these trends, we hypothesized that enterococci directly affect *C. difficile* virulence. To explore this mechanistically, we quantified *C. difficile* toxin production in the presence of enterococci in vitro. Toxin gene expression and toxin production was significantly enhanced following growth with *E. faecalis* OG1RF in liquid culture (Extended Data Fig. 3a,b). Notably, *C. difficile* toxin production was also enhanced following growth in media supplemented with cell-free supernatants from *E. faecalis*, demonstrating a role for soluble factors in enhanced virulence (Fig. 1f and Extended Data Fig. 3c). Increased toxin production was observed following exposure to a pathogenic VRE strain of *E. faecalis* (V583) (Fig. 1f and Extended Data Fig. 3c), as well as a range of *E. faecalis* and *E. faecium* strains from paediatric patients with CDI (Fig. 1g). This effect was not observed when *C. difficile* was exposed to cell-free supernatants from many non-enterococcal strains isolated from the same patients (Extended Data Fig. 3d). Together, these results illustrate that enterococci increase *C. difficile* pathogenesis by enhancing toxin production.

Enterococci reshape the metabolome

To explore the molecular mechanisms of enterococcal–*C. difficile* interactions, we performed RNA sequencing of co-cultures. *C. difficile* transcripts associated with carbohydrate uptake, amino acid utilization

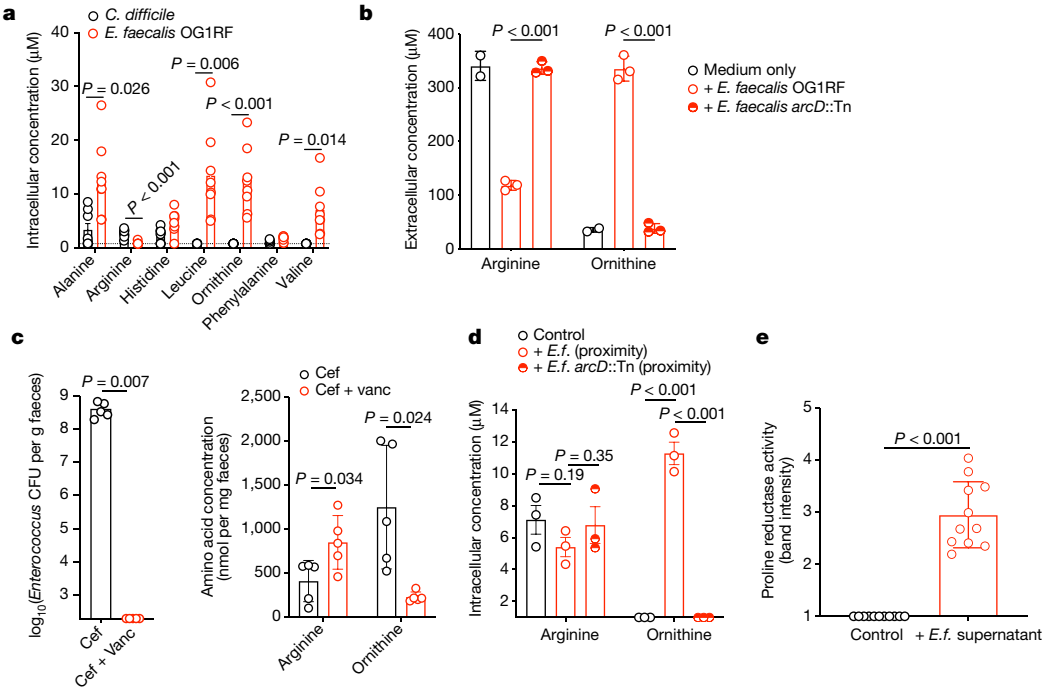

Fig. 3 | Amino acid cross-talk is central to *Enterococcus*–*C. difficile* interactions. a, Amino acid concentration in macrocolonies. Data are mean ± s.d., $n = 8$ per group; multiple two-sided *t*-tests with Bonferroni–Dunn method for correction for multiple comparisons; corrected *P* values in Supplementary Table 5. The dotted line indicates the limit of detection. **b**, Arginine and ornithine levels measured in cell-free supernatants of *E. faecalis* OG1RF or *E. faecalis* OG1RF *arcD*::Tn. Data are mean ± s.d., $n = 2$ (media only) and $n = 3$ (*E. faecalis* and *E. faecalis ArcD*::Tn); multiple two-sided *t*-tests with Bonferroni–Dunn multiple comparisons correction. **c**, *Enterococcus* burden (left) and arginine and ornithine level (right) on day of CDI quantified from faeces of mice treated with cefoperazone or cefoperazone plus vancomycin. Data are mean ± s.d., $n = 5$ per group; two-sided Mann–Whitney test for *Enterococcus* burdens; multiple two-sided *t*-tests with Bonferroni–Dunn method for multiple comparisons correction for amino acids; corrected *P* values in Supplementary Table 5. **d**, Arginine and ornithine levels quantified from *C. difficile* macrocolonies plated in the proximity of *E. faecalis* or *E. faecalis arcD*::Tn macrocolonies. Data are mean ± s.d., $n = 3$ per group; multiple two-sided *t*-tests with Bonferroni–Dunn correction for multiple comparisons; corrected *P* values in Supplementary Table 5. **e**, Band intensity of fluorescently labelled PrdA analysed by SDS–PAGE from lysates of *C. difficile* grown in fresh BHIS medium or in medium supplemented with *E. faecalis* OG1RF supernatants. Data are mean ± s.d., $n = 11$ per group; two-sided *t*-test with Welch's correction.

and Stickland fermentation were significantly altered in the presence of *E. faecalis* (Fig. 2a, Extended Data Fig. 4a and Supplementary Table 1), suggesting substantial metabolic reprogramming. Transcripts associated with metal uptake, arginine uptake and metabolism, and carbohydrate uptake and metabolism were altered in *E. faecalis* (Extended Data Fig. 4b,c and Supplementary Table 2). To contextualize these transcriptional data, we leveraged a metabolic network reconstruction[18,19] of *C. difficile* (iCdR703). Following integration of transcriptomic data[20], we generated distinct context-specific models for *C. difficile* and simulated bacterial growth (Extended Data Fig. 4d). Growth was iteratively simulated under near-optimal context-specific conditions to generate distributions of possible activity range for all metabolic reactions. Flux sampling for the biomass objective function revealed a significant increase in the predicted growth yield of *C. difficile* under co-culture conditions, suggesting that enterococci aid *C. difficile* growth (Fig. 2b). Analyses of sampled optimal metabolic flux states predicted that the core metabolism of *C. difficile* is significantly altered in the presence of enterococci and that differences in amino acid and carbohydrate-related catabolism were largely responsible for this change, with L-ornithine amino-lyase being the most important feature (Fig. 2c,d). Targeted analysis of exchange fluxes associated with substrates and by-products supported a shift to amino acid import and fermentation in co-culture (Fig. 2d and Extended Data Figs. 4a and 5a–c), with a predicted increase in uptake and consumption of ornithine, D-alanine, L-leucine and L-valine and increased efflux of the fermentation end products of isoleucine (2-methylbutyrate) and proline (5-aminovalerate) (Fig. 2e–j). Modelling also predicted increased efflux of acetate and *N*-acetyl-D-glucosamine when co-cultured (Fig. 2k,l).

On the basis of systems analyses, we predicted that *E. faecalis* reshapes the metabolic environment and acts as a source of fermentable amino acids for *C. difficile*. To validate these predictions, we measured amino acids in cells in macrocolonies. *E. faecalis* harboured high levels of fermentable amino acids predicted by our models to be important in metabolic cross-talk (Fig. 3a). We further observed that *E. faecalis* exports high levels of extracellular ornithine and depletes arginine when grown in culture (Fig. 3b). Consistent with this, mice depleted of enterococci by antibiotics harboured significantly less ornithine and enriched levels of arginine (Fig. 3c). These data suggest that *E. faecalis* is a source of several fermentable amino acids, and that ornithine and arginine are central features of metabolic remodelling. Next, we sought to determine whether ornithine is cross-fed to *C. difficile*. Ornithine quantification from macrocolonies showed that *C. difficile* cells become enriched in ornithine when grown in proximity of *E. faecalis*, demonstrating direct cross-feeding (Fig. 3d). Ornithine is a fermentable amino acid that is important for *C. difficile* persistence in the gut and can be used for both oxidative and reductive fermentative pathways[21]. Specifically, ornithine can be catabolized by *C. difficile* through the proline reductase pathway to generate energy[22]. We used an activity-based chemical probe capable of monitoring proline reductase activity[23] and observed a significant enhancement in proline reductase activity when *C. difficile* was grown in media supplemented with *E. faecalis* cell-free supernatants (Fig. 3e and Extended Data Fig. 6).

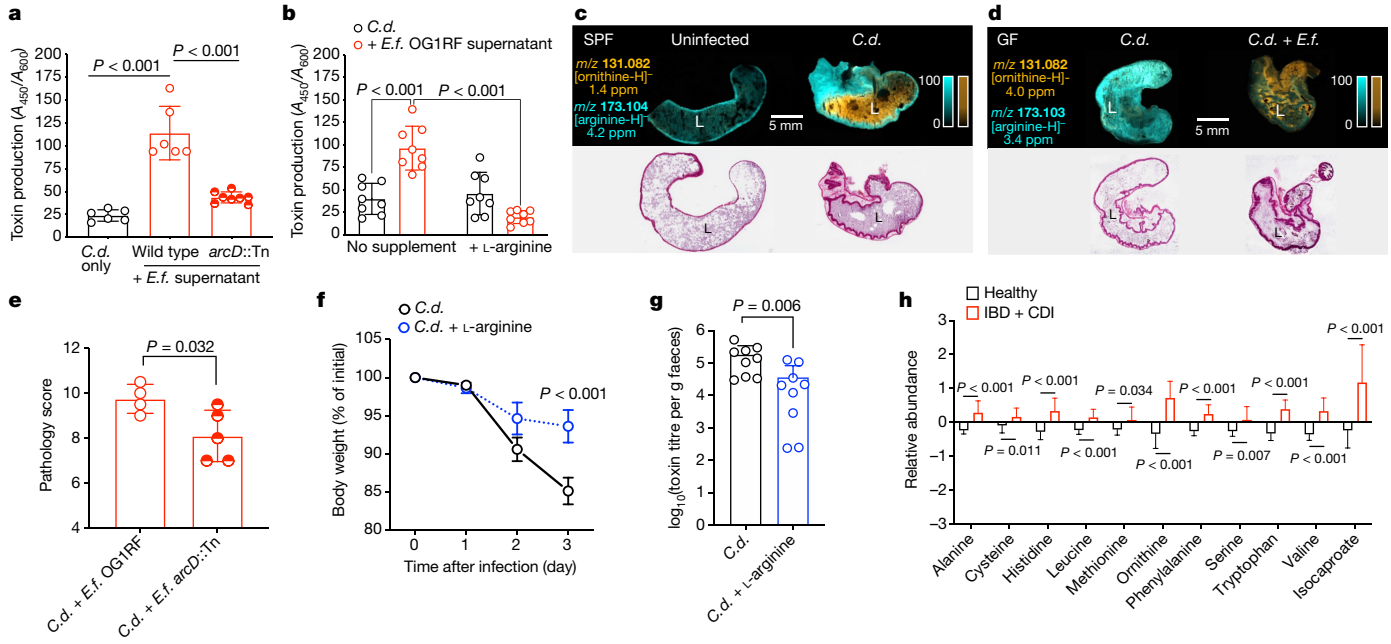

Fig. 4 | *E. faecalis* ADI pathway enhances *C. difficile* virulence. a, Toxin production by *C. difficile* CD196 grown with or without *E. faecalis* supernatants, measured by ELISA. Data are mean ± s.d., $n = 6$ (*C. difficile* only and OG1RF supernatant) and $n = 8$ (*arcD*::Tn supernatant); two-sided *t*-tests with Welch's correction. **b**, Toxin production by *C. difficile* CD196 grown with or without L-arginine supplementation. Data are mean ± s.d., $n = 8$ per group; Tukey's multiple comparison test. Corrected *P* values in Supplementary Table 5. **c**,**d**, Top, MALDI-IMS image of ornithine and arginine in uninfected or infected specific pathogen free (SPF) mice infected with *C. difficile* CD196, 3 days after infection, (**c**; representative of $n = 5$ mice) and GF mice mono-infected with *C. difficile* CD196 or co-infected with *E. faecalis* OG1RF, 2 days after infection (**d**; representative of $n = 4$ mice). Bottom, corresponding haematoxylin and eosin-stained tissue. L, lumen. **e**, Pathology score from caecum of GF mice pre-colonized with *E. faecalis* OG1RF ($n = 4$) or *E. faecalis arcD*::Tn ($n = 5$) and subsequently infected with *C. difficile*. Data are mean ± s.d.; two-sided *t*-test with Welch's correction. **f**, Weight loss of mice infected with *C. difficile* CD196 and treated with 2% L-arginine in drinking water. Data are mean ± s.d., $n = 9$ per treatment group; two-way ANOVA with Bonferroni's multiple comparison test. **g**, Faecal toxin titres from *C. difficile* in mice infected with *C. difficile* and treated with 2% L-arginine in their drinking water. Data are mean ± s.d., $n = 9$ per treatment group; two-sided Mann–Whitney test. Faecal toxin titres were measured by cytotoxicity assay. **h**, Relative abundance of selected amino acids and isocaproate in stools from paediatric healthy controls or patients with IBD and CDI. Data are mean ± s.d., $n = 20$ (patients) and $n = 19$ (controls); multiple two-sided *t*-test with Bonferroni–Dunn correction for multiple comparisons; corrected *P* values in Supplementary Table 5. Metabolites shown as relative values with each value rescaled to set the median value to 1.

This supports our modelling predictions and suggests that *C. difficile* uses *E. faecalis*-derived ornithine for energy.

The role of the ADI pathway in cross-talk

E. faecalis catabolizes arginine for energy through the arginine deiminase (ADI) pathway. During arginine uptake, ornithine is exported through the arginine–ornithine antiporter ArcD (also known as OG1RF_10103) (Fig. 3b). Ornithine is important in polymicrobial interactions in *E. faecalis*[24], and our data suggest that this amino acid is central to *C. difficile*–*E. faecalis* interactions (Figs. 2e and 3). Thus, we cultured *C. difficile* with an *E. faecalis* ArcD transposon mutant (*arcD*::Tn), which is defective in import of arginine and export of ornithine (Fig. 3b) and unable to cross-feed *C. difficile* ornithine (Fig. 3d). *C. difficile* showed a significant growth defect when grown in supernatants from *E. faecalis arcD*::Tn (Extended Data Fig. 7a), supporting a role for ornithine in fitness. Notably, enterococcal-mediated virulence enhancement in *C. difficile* was also abrogated when grown with *E. faecalis arcD*::Tn cell-free supernatants (Fig. 4a). This suggests a direct role for the enterococcal ADI system in the control of *C. difficile* virulence.

Analysis of a diverse collection of *E. faecalis* (51 genomes) and *E. faecium* (246 genomes) genomes[25,26] showed that *arcD* is present in 100% of strains. Notably, all vancomycin-resistant *E. faecium* strains that we analysed for MGE exchange during co-infection with *C. difficile* contained two copies of *arcD* located at different positions in the genome, despite the fact that *E. faecium* does not readily use arginine as an energy source[27]. These findings suggest that *arcD* is broadly conserved across clinically relevant strains of enterococci. Metagenomic analysis of adult patients with CDI[28] further showed the presence of ADI systems (*arc* genes) across an array of taxa during infection (Extended Data Fig. 7b), including the *Lachnospiraceae* and *Eggerthellaceae*. This suggests that diverse microbiota have the capacity to affect *C. difficile* growth through the action of the ADI pathway. However, enterococcal *arc* genes frequently represented most *arc* genes in patients, and enterococci were among the highest represented *arc*-containing taxa during infection (Extended Data Fig. 7b,c). To determine whether arginine depletion or ornithine production controls *C. difficile* virulence, we grew *C. difficile* in cell-free supernatants from *E. faecalis* OG1RF that had been subsequently supplemented with L-arginine. Virulence enhancement was reversed following the addition of exogenous L-arginine (Fig. 4b). Addition of L-ornithine to rich media did not lead to increased *C. difficile* toxin production (Extended Data Fig. 7d), suggesting that ornithine does not have a direct role in enhancing virulence under the tested conditions. Together, these data suggest that arginine is associated with *C. difficile* virulence and that arginine depletion by the *E. faecalis* ADI system enhances *C. difficile* virulence[29,30].

To define the role of these metabolic interactions during infection, we first performed matrix-assisted laser desorption–ionization imaging mass spectrometry (MALDI-IMS) on caeca from cefoperazone-treated mice infected with *C. difficile*, which harbour high levels of *Enterococcus* (Fig. 3c). Ornithine was seen at high abundance in the lumen following infection and arginine was reciprocally localized in tissues but absent in the lumen (Fig. 4c and Extended Data Fig. 7e). Germ-free (GF) mice mono-infected with *C. difficile* showed an influx of arginine in the lumen

and low levels of ornithine. Conversely, GF mice co-infected with *C. difficile* and *E. faecalis* were devoid of luminal arginine and had increased ornithine (Fig. 4d and Extended Data Fig. 7f–h). These data demonstrate a direct role for enterococci in substantially remodelling amino acid availability in the gut. Notably, we observed that GF mice infected with *C. difficile* had increased arginine in their caeca and faeces compared with uninfected GF mice (Extended Data Fig. 7f,h). This suggests that *C. difficile*-mediated damage to host tissue and the corresponding inflammatory response provide a nutrient source of arginine for enterococci during CDI. To test whether enterococci use arginine to thrive in the gut during CDI, we colonized conventional mice with *E. faecalis* OG1RF or *E. faecalis arcD::*Tn during CDI. *E. faecalis* lacking a functional ADI pathway (*E. faecalis arcD::*Tn) initially colonized equally well, but showed a defect in the gut during the peak of *C. difficile* disease (Extended Data Fig. 7i), demonstrating the importance of arginine in enterococcal fitness in the CDI gut. Next, to examine the role of the *E. faecalis* ArcD antiporter in promoting *C. difficile* disease, we pre-colonized GF mice with either *E. faecalis* or *E. faecalis arcD*:Cm. Depletion of arginine and accumulation of ornithine in the gut of GF mice was dependent on ArcD (Extended Data Fig. 7j,k) and *C. difficile*-infected mice with *E. faecalis arcD*:Cm showed decreased disease pathology, demonstrating the role for these metabolites in disease outcome (Fig. 4e). Finally, to confirm the role of arginine availability in CDI, we treated mice with 2% L-arginine in their drinking water. Supplementation with L-arginine did not affect the initial *C. difficile* colonization or overall burdens of enterococci, but significantly reduced toxin titres in faeces and parameters of disease severity (Fig. 4f,g and Extended Data Fig. 8a–d). Together, these observations demonstrate that enterococci modulate levels of arginine and ornithine in the gut during CDI and that arginine has a central role in *C. difficile* virulence. These findings also demonstrate that modulation of enterococcal metabolism and the nutritional landscape in the gut can alter CDI.

To demonstrate the relevance of our findings in humans, we explored the faecal metabolome of children with IBD and CDI[31]. Consistent with our findings, patients with IBD and CDI harboured significantly higher levels of fermentable amino acids—including ornithine and leucine (Fig. 4h)—and Stickland fermentation end products (Fig. 4h). We further observed a positive correlation (Spearman $\rho = 0.4243$, $n = 26$) between *C. difficile* burdens and ornithine (Extended Data Fig. 8e), supporting a key role for ornithine in CDI. Collectively, these data suggest that enterococci and *C. difficile* interact during CDI through metabolic cross-talk to support increased colonization, pathogenesis, and persistence in the gut.

Discussion

Understanding the factors that contribute to the clinical outcomes of CDI is essential for combating this urgent public health challenge. Here we show that enterococci reshape the metabolic environment in the gut to enhance *C. difficile* colonization and support fitness following disease manifestation. We propose that through the action of the ADI pathway, *E. faecalis* enhances *C. difficile* fitness via ornithine exchange, while concurrently providing metabolic cues via arginine depletion to increase virulence (Extended Data Fig. 8f). This role of enterococci in enhanced *C. difficile* toxin production is consistent with a recent study of co-infection between *C. difficile* and VRE in mice[32]. Note, however, that we performed mechanistic studies probing interactions between enterococci and *C. difficile* using *E. faecalis* strain OG1RF and *C. difficile* strain CD196 only. Although we present data that suggests that these interactions are widespread across clinically relevant enterococci, further studies that systematically test mechanisms of interaction between a diversity of enterococci and *C. difficile* strains are needed. The mechanisms by which *C. difficile* senses and responds to the enterococcal ADI pathway are not completely understood, but our data suggest a role for nutrient availability. Future studies exploring the effect of enterococcal arginine utilization on the local microenvironment during CDI are warranted, and these observations need to be extensively validated in human studies. The ability of enterococci to thrive during CDI and benefit from increased arginine availability suggests that this interaction is mutually beneficial. Although enterococci frequently dominate the microbiota during CDI and co-infection with VRE is common, it is likely that other members of the microbiota have a key role in *C. difficile* virulence[7,33]. Moreover, microbiota with ADI pathways, such as members of the *Clostridia*[34], *Lactobacillus* (Extended Data Fig. 3d), *Streptococcus*[35], and *Lachnospiraceae* (Extended Data Fig. 7b) may potentially have a similar role during infection. Together, our work demonstrates the supportive role of pathogenic microbiota in the outcome of CDI and highlights the importance of integration of metabolic signals from the microbiota in pathogen virulence. These findings have implications for our understanding of the variables affecting CDI, the risk of recurrence and the factors that influence treatment outcomes.

Online content

Any methods, additional references, Nature Research reporting summaries, source data, extended data, supplementary information, acknowledgements, peer review information; details of author contributions and competing interests; and statements of data and code availability are available at https://doi.org/10.1038/s41586-022-05438-x.

1. Abbas, A. & Zackular, J. P. Microbe–microbe interactions during *Clostridioides difficile* infection. *Curr. Opin. Microbiol.* **53**, 19–25 (2020).
2. Buffie, C. G. et al. Precision microbiome reconstitution restores bile acid mediated resistance to *Clostridium difficile*. *Nature* **517**, 205–208 (2015).
3. Lessa, F. C., Winston, L. G. & McDonald, L. C., Team, E. I. P. C. d. S. Burden of *Clostridium difficile* infection in the United States. *N. Engl. J. Med.* **372**, 2369–2370 (2015).
4. Schubert, A. M. et al. Microbiome data distinguish patients with *Clostridium difficile* infection and non-C. difficile-associated diarrhea from healthy controls. *mBio* **5**, e01021–01014 (2014).
5. Auchtung, J. M., Preisner, E. C., Collins, J., Lerma, A. I. & Britton, R. A. Identification of simplified microbial communities that inhibit *Clostridioides difficile* infection through dilution/extinction. *mSphere* **5**, e00387–20 (2020).
6. Zackular, J. P. et al. Dietary zinc alters the microbiota and decreases resistance to *Clostridium difficile* infection. *Nat. Med.* **22**, 1330–1334 (2016).
7. Tomkovich, S., Stough, J. M. A., Bishop, L. & Schloss, P. D. The initial gut microbiota and response to antibiotic perturbation influence *Clostridioides difficile* clearance in mice. *mSphere* **5**, e00869–20 (2020).
8. Berkell, M. et al. Microbiota-based markers predictive of development of *Clostridioides difficile* infection. *Nat. Commun.* **12**, 2241 (2021).
9. Antharam, V. C. et al. Intestinal dysbiosis and depletion of butyrogenic bacteria in *Clostridium difficile* infection and nosocomial diarrhea. *J. Clin. Microbiol.* **51**, 2884–2892 (2013).
10. Poduval, R. D., Kamath, R. P., Corpuz, M., Norkus, E. P. & Pitchumoni, C. S. *Clostridium difficile* and vancomycin-resistant *Enterococcus*: the new nosocomial alliance. *Am. J. Gastroenterol.* **95**, 3513–3515 (2000).
11. Ubeda, C. et al. Vancomycin-resistant *Enterococcus* domination of intestinal microbiota is enabled by antibiotic treatment in mice and precedes bloodstream invasion in humans. *J. Clin. Invest.* **120**, 4332–4341 (2010).
12. Taur, Y. et al. Intestinal domination and the risk of bacteremia in patients undergoing allogeneic hematopoietic stem cell transplantation. *Clin. Infect. Dis.* **55**, 905–914 (2012).
13. Willett, J. L. E. et al. Comparative biofilm assays using *Enterococcus faecalis* OG1RF identify new determinants of biofilm formation. *mBio* **12**, e0101121 (2021).
14. Willett, J. L. E., Robertson, E. B. & Dunny, G. M. The phosphatase Bph and peptidyl–prolyl isomerase PrsA are required for gelatinase expression and activity in *Enterococcus faecalis*. *J. Bacteriol.* **204**, e0012922 (2022).
15. Lee, I. P. A., Eldakar, O. T., Gogarten, J. P. & Andam, C. P. Bacterial cooperation through horizontal gene transfer. *Trends Ecol. Evol.* **37**, 223–232 (2021).
16. Roberts, A. P. & Mullany, P. Tn916-like genetic elements: a diverse group of modular mobile elements conferring antibiotic resistance. *FEMS Microbiol. Rev.* **35**, 856–871 (2011).
17. Chambers, C. J., Roberts, A. K., Shone, C. C. & Acharya, K. R. Structure and function of a *Clostridium difficile* sortase enzyme. *Sci. Rep.* **5**, 9449 (2015).
18. Jenior, M. L. et al. Novel drivers of virulence in *Clostridioides difficile* identified via context-specific metabolic network analysis. *mSystems* **6**, e0091921 (2021).
19. Fang, X., Lloyd, C. J. & Palsson, B. O. Reconstructing organisms in silico: genome-scale models and their emerging applications. *Nat. Rev. Microbiol.* **18**, 731–743 (2020).
20. Jenior, M. L., Moutinho, T. J., Dougherty, B. V. & Papin, J. A. Transcriptome-guided parsimonious flux analysis improves predictions with metabolic networks in complex environments. *PLoS Comput. Biol.* **16**, e1007099 (2020).
21. Pruss, K. M. et al. Oxidative ornithine metabolism supports non-inflammatory *C. difficile* colonization. *Nat Metab* **4**, 19–28 (2022).

22. Barker, H. A. Amino acid degradation by anaerobic bacteria. *Annu. Rev. Biochem.* **50**, 23–40 (1981).
23. Matthews, M. L. et al. Chemoproteomic profiling and discovery of protein electrophiles in human cells. *Nat. Chem.* **9**, 234–243 (2017).
24. Keogh, D. et al. Enterococcal metabolite cues facilitate interspecies niche modulation and polymicrobial infection. *Cell Host Microbe* **20**, 493–503 (2016).
25. Sundermann, A. J. et al. Whole genome sequencing surveillance and machine learning of the electronic health record for enhanced healthcare outbreak detection. *Clin. Infect. Dis.* **75**, 476–482 (2021).
26. Bryan, N. C. et al. Genomic and functional characterization of *Enterococcus faecalis* isolates recovered from the International Space Station and their potential for pathogenicity. *Front. Microbiol.* **11**, 515319 (2020).
27. Deibel, R. H. Utilization of arginine as an energy source for the growth of *Streptococcus faecalis*. *J. Bacteriol.* **87**, 988–992 (1964).
28. Fishbein, S. R. et al. Multi-omics investigation of *Clostridioides difficile*-colonized patients reveals pathogen and commensal correlates of *C. difficile* pathogenesis. *eLife* **11**, e72801 (2022).
29. Karasawa, T., Maegawa, T., Nojiri, T., Yamakawa, K. & Nakamura, S. Effect of arginine on toxin production by *Clostridium difficile* in defined medium. *Microbiol. Immunol.* **41**, 581–585 (1997).
30. Fredrick, C. M., Lin, G. & Johnson, E. A. Regulation of botulinum neurotoxin synthesis and toxin complex formation by arginine and glucose in *Clostridium botulinum* ATCC 3502. *Appl. Environ. Microbiol.* **83**, e00642–17 (2017).
31. Bushman, F. D. et al. Multi-omic analysis of the interaction between *Clostridioides difficile* infection and pediatric inflammatory bowel disease. *Cell Host Microbe* **28**, 422–433.e7 (2020).
32. Keith, J. W. et al. Impact of antibiotic-resistant bacteria on immune activation and *Clostridioides difficile* infection in the mouse intestine. *Infect. Immun.* **88**, e00362–19 (2020).
33. Lesniak, N. A. et al. The gut bacterial community potentiates *Clostridioides difficile* infection severity. *mBio* **13**, e0118322 (2022).
34. Girinathan, B. P. et al. In vivo commensal control of *Clostridioides difficile* virulence. *Cell Host Microbe* **29**, 1693–1708.e1697 (2021).
35. Hirose, Y. et al. *Streptococcus pyogenes* upregulates arginine catabolism to exert its pathogenesis on the skin surface. *Cell Rep.* **34**, 108924 (2021).

Methods

Bacterial strains and growth conditions

Strains used in this study are listed in Supplementary Table 3[36–38]. *C. difficile, Enterococcus* and *E. coli* strains were grown at 37 °C in an anaerobic chamber (85% nitrogen, 10% hydrogen, 5% carbon dioxide; Coy Lab Products) in brain-heart-infusion broth (BD Life Sciences) supplemented with 0.5% yeast extract (BD Life Sciences) and 0.1% L-cysteine (Sigma-Aldrich) (BHIS) unless otherwise stated. For bacterial growth curves, *C. difficile* were incubated with double orbital shaking at 37 °C and A_{600} was measured every 30 min in a BioTek Epoch 2 (BioTek). For growth in presence of *E. faecalis* supernatants, cultures were normalized to optical density and sub-cultured (1:100) into 200 µl fresh BHIS with 70% *E. faecalis* supernatants in a 96-well plate sealed with a gas-permeable membrane (Breathe-Easy) (Millipore-Sigma). Sequence-defined transposon mutants used in this study were confirmed using gene specific primers[39].

Quantification of *C. difficile* toxin production

For quantification of *C. difficile* toxin from culture, *C. difficile* was grown for 24 h anaerobically, pelleted at 4,000*g* for 10 min, and filtered through a 0.2 µm filter. For quantification of toxin via ELISA, the *C. difficile* Tox A/B II ELISA (Meridian Bioscience) was used per manufacturer's instruction. For quantification of *C. difficile* toxin titres via cytotoxicity assay, a Vero cell-rounding cytotoxicity assay was used as previously described[6]. In brief, Vero cells (ATCC #CCL-81) were plated at 1×10^4 cells per well in a 96-well flat bottom cell-culture treated microtiter plate and incubated for 16–24 h. *C. difficile* filtered supernatants were titrated in tenfold dilutions to a maximum dilution of 10^{-8}. After an overnight incubation, Vero cell rounding was assessed under 10× magnification. Cytotoxicity data are expressed as the reciprocal value of the highest dilution that rounded 100% of the cells. For co-culture growth, toxin levels were normalized to *C. difficile* CFU. For cultures grown with *Enterococcus* cell-free supernatants, toxin levels were normalized to *C. difficile* A_{600}. When grown in the presence of *Enterococcus* supernatants, *C. difficile* was grown in 70% cell-free supernatants and 30% fresh media. The ADI pathway leads to production of ammonia and alteration in pH in some pathogens[35]; however, adjustment of pH in *E. faecalis* supernatants did not directly lead to a significant impact on toxin output in our assay. All toxin quantification assays were independently replicated at least three times and representative assays are shown.

Co-culture growth assays on solid media

For macrocolonies, E. faecalis and C. difficile overnight cultures were normalized based on A_{600} and 10 µl were plated onto BHIS + L-cysteine agar plates and grown for 7 days to produce macrocolonies. For proximity assays to measure metabolite exchange, cultures were normalized by absorbance, and 10 µl were spotted onto BHIS + L-cysteine agar plates at a 1.5 cm distance and physical mixing of cells was avoided. Macrocolony cultures were grown for 7 days.

Animal and experimental models of CDI

Animal experiments were approved by the Animal Care and Use Committees of Vanderbilt University, the Children's Hospital of Philadelphia, and the University of Pennsylvania Perelman School of Medicine (protocols M1700053, IAC 18-001316, 806279). For CDI in conventional facilities, 4- to 8-week-old C57BL/6 male mice were purchased from Jackson Laboratories and given one week to equilibrate their microbiota prior to experimentation. All experimental manipulations were performed in a biosafety level 2 laminar flow hood. Mice were housed in individual cages under the same conditions during the experiment, investigators were not blinded to treatment groups, and all mice were culture-negative for *C. difficile* prior to infection. For the CDI in conventional mice, the mice were given antibiotics (0.5 mg ml^{-1} cefoperazone or 0.5 mg ml^{-1} cefoperazone + 1 mg ml^{-1} vancomycin) in drinking water ad libitum for 5 days followed by a 2-day recovery period and subsequent infection as previously described[6,40]. Mice were infected via oral gavage with 1×10^5 spores of *C. difficile* resuspended in sterile PBS. *C. difficile* strains CD196, M7404, and M7404 TcdA$^-$ TcdB$^-$ were used for conventional infections, as described in the text. When noted, mice were co-infected with 5×10^8 *E. faecalis* (wild-type strain OG1RF or *arcD*::Tn) cells. *E. faecalis* cells were grown to stationary phase, washed in PBS twice prior to infection, and gavaged prior to infection with *C. difficile* spores. For *C. difficile* infection in GF mice, 6-week-old C57BL/6 female mice were used and mice were infected with either 1×10^5 spores of *C. difficile* (strain CD196) or *C. difficile* spores + 5×10^8 *E. faecalis* (wild-type strain OG1RF or *arcD*::Tn) cells in PBS. Both conventional and GF mice were monitored for survival and were euthanized after reaching a terminal endpoint of appearing moribund or experiencing weight loss >20% from baseline. *C. difficile* and enterococcal CFUs were quantified daily from faecal samples. All samples were collected and all stool-related data are reported, unless mice were too unwell to acquire a fresh stool sample. Samples were diluted and homogenized in PBS and serially plated onto taurocholate cycloserine cefoxitin fructose agar (TCCFA) for *C. difficile* and bile esculin agar for enterococci. Wild-type *E. faecalis* OG1RF was grown on BHI agar with rifampicin (200µg ml^{-1}), and transposon mutants were grown on BHI agar with rifampicin and chloramphenicol (10µg ml^{-1}).

Histological analysis

At necropsy, caeca and colons were collected, fixed in 10% formalin solution and embedded in paraffin. Sections were stained with haematoxylin and eosin. Each section was given a disease score by a pathologist in a blinded manner based on previously described criteria[40]. Histological scores were reported as a cumulative score of three independent scoring criteria: inflammation, oedema and epithelial cell damage.

C. difficile toxin titres from faeces

C. difficile toxin cytotoxicity was determined using a Vero cell-rounding cytotoxicity as described above. Fresh faecal samples were homogenized in 1 ml of sterile PBS and pelleted at 4,000*g* for 5 min. The supernatants were filtered through a 0.2-µm filter and titrated in tenfold dilutions within the wells to a maximum dilution of 10^{-8}. After an overnight incubation, Vero cell rounding was assessed under 10× magnification. Cytotoxicity data are expressed as the reciprocal value of the highest dilution that rounded 100% of the cells per gram of sample.

Quantification of *C. difficile* and enterococci from human stool samples

Bacterial burdens were quantified from frozen stool from the two patient cohorts as CFUs per gram of stool. Samples were weighed and homogenized in sterile PBS. The samples were then serially diluted and plated on differential media. Enterococci were isolated in aerobic conditions by plating on bile esculin agar (BD, 221409) and visually differentiated from streptococci by blackening around colonies from the esculetin reaction with iron salts in the media and confirmed by 16S rRNA gene sequencing. *C. difficile* was plated on TCCFA in anaerobic conditions.

DNA isolation and 16S rRNA gene sequence analysis for bacterial identification

Genomic DNA from *C. difficile* and enterococci bacterial isolates were extracted from frozen pellets. Prior to extraction, the cell pellets were mechanically lysed in a PowerLyzer Homogenizer (Qiagen) with 0.1 mm glass beads. DNA was extracted using the DNeasy Blood and Tissue kit with QIAcube automation according to the manufacturer's instructions (Qiagen). The 16S rRNA gene was amplified using universal 27F and 1492R primers. All PCR products were purified with the Monarch PCR & DNA Cleanup kit (New England Biolabs) and sequenced by Sanger DNA sequencing performed by CHOP's Nucleic Acid PCR Core Facility.

The first 50 bases and everything after 850 bases were trimmed from the 5′ end of each sequence and sequence analysis was carried out by NCBI BLASTn similarity search within the 16S ribosomal database with an E-value cut-off of 0.01. Enterococci were identified on the parameters of highest per cent identity and agreement between forward and reverse sequences.

Quantifying *C. difficile* survival in antibiotic-treated interspecies biofilms

The biofilm protocol was adapted from Kumar et al.[41]. Absorbance-normalized liquid cultures of *C. difficile* CD196, *E. faecalis* OG1RF (isogenic wild-type and noted transposon mutants)[13,39], and *E. coli* DH5α were seeded in monoculture or in co-culture with CD196 in BHIS+ L-cysteine media in non-treated 24-well microplates. Biofilms were incubated for 4 days anaerobically at 37 °C. All non-adherent cells were washed with PBS buffer and the cells in biofilms were treated with fresh BHIS media or fresh BHIS media with vancomycin at 5 μg ml^{-1}. After overnight vancomycin treatment, all treatment media was removed from the wells and replaced with 1 ml fresh BHIS. Biofilms were then scraped into solution using a sterile pipette tip. A tenfold dilution series was prepared, and spot plated in 5 μl quantities onto TCCFA. CFU counts were determined by counting bacterial colonies on the agar plate from the serial dilution. Biofilm assays were independently replicated at least three times and representative assays are shown in figures.

FISH

FISH for *C. difficile* and *Enterococcus* was performed on paraffin-embedded 5-μm caecal sections from *C. difficile*-infected mouse tissues. Embedded tissues were deparaffinized using 2 washes with xylene, 2 washes with 100% ethanol, and a single wash with sterile water. Hybridization was performed overnight (16 h) at 46 °C concurrently with both fluorescently labelled oligonucleotide probes at 5 ng ml^{-1} in hybridization buffer with 35% formamide. Following hybridization, slides were washed for 40 min with prewarmed wash buffer at 48 °C. Prior to imaging, VectaShield with DAPI was added to the slide to protect from photobleaching and a coverslip was placed prior to imaging. Imaging was performed using super resolution structured illumination microscopy imaging at the Vanderbilt University Cell Imaging Shared Resource. Maximum intensity projections of 6.8 mm *z*-stacks are presented. Images were denoised using NIS Elements Artificial Intelligence Denoise.AI capabilities. Brightness and contrast were adjusted consistently for optimum visualization. HPLC-purified probes for *C. difficile* (Cy5–CATCCTGTACTGGCTCAC)[42] and *Enterococcus* (Cy3–CACC GCGGGTCCATCCATCA)[43] with 5′ fluorophores were acquired from Integrated DNA technologies (IDT). *Enterococcus* was false-coloured green in micrographs to provide greater contrast against *C. difficile* cells. FISH assays were independently replicated in five mice and representative images are shown in figures.

RNA sequencing

Bacterial growth and RNA extraction. Absorbance-normalized cultures of *C. difficile* strain CD196, *E. faecalis* strain OG1RF, and mixed co-cultures were grown anaerobically in biological triplicate in BHIS + L-cysteine at 37 °C for 4 h (exponential phase). For co-cultures, *C. difficile* was seeded at a 2:1 ratio to *E. faecalis* to account for differences in growth rates between species. After growth, a 1:1 solution of acetone:ethanol was added to an equal volume of the culture. Samples were stored at −80 °C until used for RNA extraction, and RNA extraction was performed as previously described[44]. RNA was quantified and either used for RNA sequencing or quantitative PCR (qPCR) as described below.

Library construction. RNA-seq library construction and sequencing were performed by HudsonAlpha Institute for Biotechnology. The concentration and integrity of extracted total RNA were estimated by a Qubit 2.0 Fluorometer (Invitrogen) and an Agilent 2100 Bioanalyzer (Applied Biosystems), and 500 ng of RNA was utilized for downstream applications. rRNA was removed using the Ribo-Zero Gold (Epidemiology) kit (Illumina) according to the manufacturer's instructions. RNA was fragmented and primed for first-strand synthesis using the NEBNext first-strand synthesis module (New England BioLabs). Directional second-strand synthesis was performed using the NEBNext Ultra Directional second-strand synthesis kit. Libraries were then prepared from samples using the NEBNext DNA Library Prep master mix set (Illumina) with the following slight modifications. End repair was performed and followed by polyadenylic acid (poly[A]) addition and custom adapter ligation. Ligated samples were individually barcoded with unique in-house Genomic Services Lab (GSL) primers and amplified through 12 cycles of PCR. Library quantity was assessed by a Qubit 2.0 Fluorometer, and the library quality was assessed by utilizing a DNA High Sensitivity Chip on a Caliper GX (PerkinElmer). The qPCR-based Kapa Biosystems library quantification kit (Kapa Biosystems) was used for final accurate quantification of libraries prior to sequencing. Each library was diluted to a final concentration of 12.5 nM and pooled equimolar prior to clustering. Paired-end sequencing was performed on an Illumina HiSeq2500 sequencer (Illumina). Raw RNA-sequencing data and processed data are deposited in the NCBI Gene Expression Omnibus (GEO) under accession number GSE165751.

RNA-seq analysis. Single-end RNA-seq reads were trimmed of any adaptor sequences with trim-galore (version 0.6.6). The remaining reads were aligned to the *C. difficile* reference genome using STAR (version 2.7.6a) with the following parameters: --outSAMtype BAM SortedByCoordinate --limitBAMsortRAM 1500000000 – outSAMmapqUnique 255 –outFilterMultimapNmax 1 –alignIntronMax 1. Reads count on each gene were calculated at the same time of mapping with the parameter – quantMode GeneCounts.

Differential expression analysis between co-culture vs *C. difficile* alone was done using R package DESeq2 (version 1.30.0) and the Wald test. The read counts were normalized among the samples and were transformed to log2 form using the variance stabilizing transformations (VST) method. Volcano plot was drawn using the R package EnhancedVolcano (version 1.8.0). Only the differentially expressed genes (adjusted p-value < 0.01 and fold change ≥ 2) were shown on the plot, amino acid metabolism-associated genes were coloured in red and only the genes with classic nomenclatures were labelled. Pathways were assigned for differentially expressed genes based on KEGG database.

Genome-scale metabolic network reconstruction analysis

Genome-scale metabolic network reconstruction (GENRE) for *C. difficile* R20291 (iCdR703) was used for analysis of transcriptional data from RNA-seq. Although designed for *C. difficile* strain R20291, iCdR703 contains identical components for *C. difficile* strain CD196[18]. *C. difficile* GENRE (iCdR703) was accessed from (https://github.com/mjenior/Smith_etal_Enterococcus) and exchange reaction bounds were set to simulate rich BHI medium conditions. Transcriptomic read abundances were evenly subsampled between experimental replicates and each replicate was integrated individually, creating multiple unique models of context-specific metabolism for which all observed variation in structure and activity was then collapsed within experimental groups to obtain a more comprehensive model of metabolism for each. Transcriptomic data integration and context-specific model generation were performed with RIPTiDe (v3.3.6) on the default settings[20]. Context-specific flux sampling results were subsequently analysed in R (v3.2.0) with the vegan[45] and AUCRF[46] packages. Specifically, the AUCRF package was used for Random Forest machine learning functions with an increment of removing 1 variable at a time during each test phase (pdel = 0) with a minimum number of variables to include in the final model of 10 (k_0 = 10), and an initial seed of 906801. The metabolic network reconstruction of *C. difficile* (iCdR703) was generated to

represent active metabolism in both in vitro and infection settings, as described previously[18].

Quantitative PCR

RNA concentration was determined using Synergy 2 with Gen 5 software (BioTek) and 2 µg was reverse transcribed by M-MLV reverse transcriptase (Fisher Scientific) in the presence of RNase inhibitor (Promega) and random hexamers (Promega). Reactions lacking the reverse transcriptase were used to control for DNA contamination. Newly created cDNA was diluted 1:100 and used in quantitative PCR with reverse transcription using iQ SYBR green supermix (Bio-Rad). Amplification was achieved using a 3-step melt cure program on a CFX96 qPCR cycler (Bio-Rad). Transcript abundance was calculated using the $\Delta\Delta C_T$ method normalized by the *C. difficile rpoB* gene and performed in biological triplicates. Each assay was repeated three independent times and a representative independent experiment is shown.

Metabolomics analyses

For targeted metabolomics analysis of amino acids in sterile, spent bacterial culture supernatants, *C. difficile* CD196 and *E. faecalis* OG1RF were grown in BHIS media, sub-cultured 1:100 into BHIS, and grown for 20 h under anaerobic conditions. Cultures were then centrifuged at 4,000 r.p.m. for 10 min and filter sterilized with 0.22-µm filters. Cell-free culture supernatants were supplemented with fresh, sterile BHIS media to generate 70% conditioned media. For targeted analyses of amino acids in faecal samples, samples were weighed and homogenized in sterile PBS. Contents were sterilized with 0.22-µm filters. For targeted analyses of macrocolonies, colonies were scraped from agar and cell lysates were analysed. Analysis was performed by the Microbial Culture and Metabolomics Core of the PennCHOP Microbiome Program. Amino acids were quantified using a Waters Acquity uPLC System with an AccQ-Tag Ultra C18 1.7 µm, 2.1 × 100 mm column and a photodiode detector array. Bacterial culture samples were centrifuged at 13,000*g* for 5 min, and the supernatant was transferred to a new tube and centrifuged again at 13,000*g* for 5 min. Amino acids in the supernatant were derivatized using the Waters AccQ-Tag Ultra Amino Acid Derivatization Kit (Waters Corporation) and analysed using the UPLC AAA H-Class Application Kit (Waters Corporation) according to manufacturer's instructions. Quality control checks (blanks and standards) were run every eight samples. All chemicals and reagents used were mass spectrometry grade.

Imaging mass spectrometry analyses

Bacterial colonies grown on agar as previously described to be analysed via MALDI-IMS were mounted onto indium tin oxide-coated microscope slides. These slides were placed in slide boxes, shipped to the University of Florida on dry ice, and then stored at −80 °C until analysis. After removal from the freezer, colony samples are dried in a desiccator at room temperature for 2–3 days prior to drying in a custom-built vacuum drying chamber (160 mtorr, room temperature, 1 h) to remove moisture and facilitate adherence of the agar to the microscope slide. A 9-aminoacridine (9AA) MALDI matrix layer was applied using a custom-built sublimation apparatus (<50 mtorr, 180 °C, 14 min, resulting in ~3 mg of matrix deposited on the slide)[47].

Tissue samples to be analysed by MALDI-IMS were embedded in OCT, shipped to the University of Florida on dry ice, and stored at −80 °C until analysis. Tissue sections were prepared at 12 µm thickness using a Leica CM 3050S Research Cryostat (Leica Biosystems) (−30 °C object temperature, −28 °C chamber temperature) and thaw mounted onto indium tin oxide-coated microscope slides. Samples to be compared via IMS were mounted on the same microscope slide to ensure identical sample preparation and facilitate accurate metabolite comparisons between tissue types. Slides with mounted tissue sections were then warmed to room temperature in a desiccator for ~30 min before application of a 1,5-diaminonapthalene MALDI matrix layer using the sublimation apparatus (<50 mtorr, 120 °C, 11 min, resulting in ~3 mg of matrix deposited on the slide)[48]. A recrystallization procedure was performed following matrix application to enhance analyte extraction into the MALDI matrix layer (200 µl methanol, 60 °C, 2 min)[49].

All imaging mass spectrometry experiments were performed in negative ion mode on a 7T Fourier transform ion cyclotron resonance (FT-ICR) mass spectrometer equipped with a dynamically harmonized ParaCell (Bruker Daltonics). The instrument contains an Apollo II dual MALDI/ESI source that uses a Smartbeam II Nd:YAG MALDI laser (2 kHz, 355 nm). Images were acquired at a pixel spacing of 100 µm in both the *x* and *y* dimensions using a ~25-µm laser beam and a 90-µm Smart Walk (500 laser shots). Continuous accumulation of selected ions (CASI) was employed to improve the sensitivity of selected metabolites by setting the Q1 mass to *m/z* 140 and the mass window[50] to 90 *m/z*. Co-culture data were collected from *m/z* 100 to 1,000 using a 0.9787 s time-domain transient length, resulting in a resolving power of ~228,000 at *m/z* 122. Tissue data were collected from *m/z* 100 to 1,000 using either a 0.2447 s or 0.4893 s time-domain transient length, resulting in a resolving power of ~84,000 or ~169,000 (at *m/z* 156), respectively. Internal calibration (quadratic fit for full spectrum data and single point correction for CASI data) was performed using matrix-related ions. Ion images were visualized using FlexImaging 5.0 (Bruker Daltonics). Ion images are displayed without normalization and using interpolation. Following image acquisition, tissue sections were stained using haematoxylin and eosin, scanned using an Aperio Scanscope CS (Leica Biosystems) bright field whole slide scanner, and visualized using Aperio ImageScope (Leica Biosystems).

In situ labelling of *C. difficile* with a hydrazine probe and gel-based profiling of D-proline reductase activity

A phenylhydrazine probe was synthesized according to the literature[23]. Working stock solutions (0.1 mM) were prepared in H_2O containing 10% dimethyl sulfoxide (DMSO) and neutralized to pH 6.0–7.0 and stored at −80 °C prior to use.

Probe treatment and gel-based analysis of probe-labelled proteins was adapted and optimized following a previous study[23]. In brief, cultures were collected (4,000*g*, 10 min, 4 °C) and resuspended in 1 ml of growth medium. Cells were treated with the hydrazine probe (1 mM) and incubated anaerobically for 30 min at 37 °C. The cells were washed by centrifugation (17,000*g*, 3 min, 4 °C) and resuspended in ice-cold deoxygenated PBS. Cell pellets were stored at −80 °C prior to use.

Pelleted *C. difficile* cells were resuspended in 8 M urea in PBS (400 µl), incubated on ice for 30 min and lysed with a Branson SFX250 Sonifier equipped with a 102C (3 × 10 pulses, 0.3 s on and 2 s off, 15% energy). Soluble proteomes were fractionated by centrifugation (100,000*g*, 30 min, 4 °C) and total protein concentrations were determined using the DC protein assay (Bio-Rad Laboratories) on a microplate reader (Biotek ELx808).

A freshly prepared copper (I)-catalysed azide alkyne cycloaddition (CuAAC (click)) reagent mixture (6 µl) containing 3 µl of 1.7 mM Tris(benzyltriazolylmethyl)amine (TBTA) in DMSO:*t*-butanol (1:4 v/v), 1 µl of 50 mM $CuSO_4$ in H_2O, 1 µl of 1.25 mM rhodamine-azide (Rh-N_3) in DMSO, and 1 µl of freshly prepared 50 mM tris(2-carboxyethyl) phosphine (TCEP) in H_2O was added to samples (50 µl) containing the probe-labelled proteomes (1 mg ml^{-1}). After addition of the click mixture, samples were vortexed and incubated at room temperature for 1 h while rotating and quenched by addition of 17 µl of 4× SDS loading buffer. Probe-labelled proteins were resolved by SDS–PAGE and visualized by in-gel fluorescence scanning on a ChemiDoc MP Imaging System (Bio-Rad Laboratories). D-Proline reductase (0.3 mg ml^{-1}), as purified below, was incubated with the phenylhydrazine probe (3 µM, 15 min, at 37 °C), conjugated to Rh-N_3 and compared against *C. difficile* gel profiles to identify active PrdA.

Band intensities of the active (probe-labelled) PrdA subunit of D-proline reductase were quantified using ImageJ Software[51] and normalized against corresponding expression profiles.

Purification of D-proline reductase from *C. difficile*

The purification of D-proline reductase was adapted from a previous study[52]. *C. difficile* VPI 10463 was cultivated in rich growth medium containing 20 g l^{-1} tryptone (dot scientific), 10 g l^{-1} yeast extract (Acros Organics, 451120050), 1.75 g l^{-1} K_2HPO_4 (Fisher), 1 μM selenite (Honeywell) and supplemented with 40 mM L-proline (Alfa Aesar) and 40 mM L-alanine (Alfa Aesar) to enhance the expression of *prd* at 37 °C. After 24 h, cells were collected by centrifugation (5,000*g*, 30 min, 4 °C), flash-frozen in liquid N_2 and stored at −80 °C. The cell paste (8–10 g per l culture) was resuspended (5 ml per g paste) in 50 mM Tris buffer (pH 8.4) containing 1 mM Ethylenediaminetetraacetic acid (EDTA), and 1 mM dithiothreitol (DTT) at 4 °C, lysed by sonication (1 s on and 2 s off for 10 min, 40% amplitude) on Qsonica Q700 sonicator and centrifuged (30,000*g*, 20 min, 4 °C). Stepwise ammonium sulfate fractionation (25, 40, 60 and 85% saturation) was performed to isolate D-proline reductase-containing fractions. In brief, solid ammonium sulfate (Alfa Aesar) was slowly added to the lysate stirring at 4 °C to create a 25% saturated solution. After 1 h, precipitated proteins were collected by centrifugation (30,000*g*, 20 min, 4 °C). Steps were repeated on the remaining supernatant to fractionate precipitated proteins at 40, 60 and 85% ammonium sulfate saturation. D-Proline reductase was precipitated in 40–60% ammonium sulfate. The precipitate was solubilized in 50 mM Tris buffer (pH 8.4) containing 1 mM EDTA, 1 mM DTT, and 2 M ammonium sulfate and loaded onto a phenyl-Sepharose column (20 × 2.5 cm) equilibrated in the same buffer. The column was washed with equilibration buffer until absorption of the eluate at 280 nm (A_{280}) and 260 nm (A_{260}) was ~0 (~5 column volumes). Bound proteins were eluted by a 400-ml linear gradient of ammonium sulfate (2.0 M to 0.0 M) in 50 mM Tris buffer (pH 8.4) containing 1 mM EDTA and 1 mM DTT. Fractions containing D-proline reductase as determined by SDS–PAGE were pooled and dialysed against 50 mM Tris buffer (pH 8.4) containing 1 mM DTT and 250 mM NaCl for 12 h at 4 °C. The protein was concentrated to ~4 mg ml^{-1} in 10% glycerol and flash-frozen at −80 °C. The yield for D-proline reductase complex was 3 mg of protein per g cell paste. The active protein was confirmed by LC–MS/MS.

16S rRNA gene sequencing and analysis

Specimens positive for *C. difficile* toxin A or B by enzyme immunoassay (EIA) were captured from a cross-sectional study of human subjects (University of Pennsylvania IRB no. 826543). We extracted DNA from residual faeces using the Powersoil kit (Qiagen), amplified the V1–V2 hypervariable region of the 16S rRNA gene using barcoded 27F and 338R primers, and performed paired-end 250bp sequencing (Illumina MiSeq). Sequences were demultiplexed and aligned with QIIME2; sequence denoising and amplicon sequence-variant (ASV) binning was performed with DADA2. Taxonomic assignment was performed by basic local alignment (BLAST) to the SILVA rRNA gene database (version 132). Linear regression relating subjects' peripheral WBC count to $\log_{10}$ *Enterococcus* relative abundance performed using R statistical software (version 4.1.0). *Enterococcus* abundance values of zero, which cannot translate to the log scale, were treated as the lowest observed *Enterococcus* abundance.

Identification of shared sequences present in vancomycin-resistant enterococci and *C. difficile* genomes

We used a previously developed approach[53] to scan the genomes of clinical bacterial isolates collected from hospital-associated infections at the University of Pittsburgh Medical Center for highly similar nucleotide sequences present in the genomes of different species[25]. We identified nucleotide sequences >5kb that were present at 99.98% identity or greater (that is, no more than 1 mutation per 5kb of sequence) in both VRE and *C. difficile* genomes. Shared sequences were annotated with Prokka[54] and were compared to one another, and to publicly available genomes, with BLAST. Share sequence clusters were visualized with Cytoscape[55]. MGE clusters are available in Supplementary Table 4 and FASTA files available in the Supplementary Information.

Expression of collagen adhesin in *E. faecalis*

The predicted coding sequence and ribosome-binding region of the CD0386-like surface adhesin was amplified from the vancomycin-resistant *E. faecium* isolate VRE33574 by PCR, and was cloned into the pMSP3535 expression vector using Gibson assembly[56]. The resulting vector was transformed into *E. faecalis* strain OG1RF, and transformants were selected with 15 μg ml^{-1} erythromycin. Transformants were tested for their ability to form biofilms on standard and collagen-coated plates following a previously described protocol[57]. In brief, overnight cultures were diluted 100-fold into BHI broth supplemented with 0.25% glucose; 200 μl of each culture was plated into 8 replicate wells of a 96-well untreated polystyrene microtitre plate, and plates were incubated for 24 h at 37 °C under static conditions. Plates were washed three times with 250 μl 1× phosphate-buffered saline (PBS) to remove unattached cells, and then wells were stained with 200 μl of 0.1% crystal violet in water. After incubation for 30 min at 4 °C, stained wells were washed twice with 250 μl of 1× PBS to remove excess stain. Plates were dried, and then 250 μl of 4:1 ethanol:acetone was added to each well to solubilize the crystal violet-stained biofilm. After incubation for 45 min at room temperature, the absorbance of the dissolved crystal violet was measured at 595 nm using a Synergy H1 microplate reader (Biotek). Adhesin expression was induced with 25 ng ml^{-1} nisin, and a transformant carrying the empty pMSP3535 vector was used as a comparison strain.

Analysis of ArcD conservation in the human microbiome

Raw reads from an adult CDI metagenomics dataset[28] were aligned to all prokaryote proteins in KEGG using Diamond (v2.0.14). Reads aligned to any of the *arc* operons (*arcA*, *arcB*, *arcC*, *arcD/arcF*, and *arcR* with KO ids K01478, K03758, K24446, K00926, K21827, K21828, K00611, K09065) were filtered out from the original fastq files, and the DNA sequences were then taxonomically classified using Kraken2 (v2.1.2). The normalized read counts for selected taxa were used to generate the heat map. After reads were directly assigned a taxonomy using Kraken2, they were analysed and visualized in R (version 3.5.2). Relative abundances were calculated by aggregating read counts at the family level and below and dividing by total number of classified reads per sample. We focused on adults with symptomatic adult CDI (n = 48). The top 10 bacterial families containing *arc* operon mapping reads are visualized in Extended Data Fig. 7b,c. The conservation of *arcD* in enterococci was determined by pangenome analysis of previously published *E. faecalis* and *E. faecium* genomes[25,26]. In both cases, gene presence/absence matrices previously constructed with Roary[58] were queried for *arcD*. Among 51 genetically diverse *E. faecalis* isolate genomes, *arcD* was found in all genomes. Among the 246 vancomycin-resistant *E. faecium* genomes used for shared sequence analysis, all genomes were found to encode two copies of *arcD* located at different positions in the genome.

Human samples

Vanderbilt University Medical Center. Paediatric participants, aged 12 months to 18 years, were prospectively enroled from July 2017 through December 2019 at Monroe Carell Jr Children's Hospital at Vanderbilt after informed parental consent and patient assent when applicable. This study was approved by the Vanderbilt Institutional Review Board (IRB no. 170067). Thorough medical histories were obtained from all participants, including past hospitalizations, surgeries, and medications received 30 days prior to enrolment and confirmed by medical record review. Data were kept strictly confidential using a REDCap database (REDCap software, Vanderbilt University)[36–38,59]. Symptomatic *C. difficile* cases where children with diarrhea (unformed stool) between 12 months and 18 years of age who underwent clinical laboratory testing

and tested positive for *C. difficile* by nucleic acid amplification-based testing (NAAT). *C. difficile* negative children (confirmed by NAAT) included children with cystic fibrosis, inflammatory bowel disease, and cancer. No images of human subjects are included in the figures, extended data, or supplementary materials.

Children's Hospital of Philadelphia. Subjects were recruited at the Children's Hospital of Philadelphia (CHOP) from September 2015 to April 2018 and informed consent was acquired (IRB approval number 15-011817), as previously described[31]. Groups included healthy children and children with IBD and concurrent CDI. Healthy children were age-matched to those with IBD and CDI. For inclusion in the *C. difficile*-infected group, patients needed to (1) have an underlying diagnosis of inflammatory bowel disease (2) have loose, watery stool at least 3 times per day for >24 h or an increase in stool frequency from baseline, and (3) be positive by glutamate dehydrogenase testing assay or PCR for the presence of the toxin A/B gene (cycle of threshold <40). Clinical manifestations of CDI ranged from mild diarrhea to fulminant colitis and shock. Patients with CDI were identified by notification of positive testing for toxigenic *C. difficile* by the CHOP Microbiology laboratory. Exclusion criteria included history of haemophagocytic lymphohistiocytosis or Langerhan's cell histiocytosis or concurrent gastrointestinal infection proven by clinical testing. Prior history of *C. difficile* or recent antibiotic use were not exclusion criteria. Inclusion criteria for healthy controls included if they did not have a chronic diagnosis and could provide stool samples at all three time points. Healthy children were excluded if they had diarrhea, antibiotic use in 90 days prior to enrolment, or a family member with *C. difficile* enroled into the study. Patients with CDI were included with either primary infection or recurrent infections. There were 10 out of 23 patients in the IBD plus CDI cohort who had recurrent CDI at enrolment, three of whom had a prior positive clinical test for *C. difficile* within three months of enrolment. Untargeted metabolomics on the stool samples from these patients was performed as previously described[31]. No images of human subjects are included in the figures, extended data or Supplementary Information.

The Hospital of the University of Pennsylvania. Subjects with positive testing by enzyme immunoassay (EIA) for *C. difficile* toxin A or B were identified over six months of continuous screening (February–August 2017) at the Hospital of the University of Pennsylvania, with a waiver of informed consent granted by the University of Pennsylvania Institutional Review Board (IRB no. 826543). Faecal specimens from 50 consecutive toxin EIA-positive subjects underwent 16S rRNA gene sequencing as described above, and the faecal bacterial community composition was compared to the maximum peripheral WBC count within 72 h of the index *C. difficile* test. Samples in which there were no detected *Enterococcus* reads were assigned the minimum observed value in the data. WBC data were extracted from the subjects' electronic medical records. No images of human subjects are included in the figures, extended data, or Supplementary Information.

Statistical analyses

Statistical analyses were performed using GraphPad Prism version 8 and R version 3.5.2. Specific statistical tests, replicate numbers, calculated errors and extended information for each experiment are reported in the figure legends. All data represent distinct samples unless otherwise stated (for example, longitudinal bacterial burdens in faeces).

Materials availability

All strains and materials used in this study are available upon request.

Reporting summary

Further information on research design is available in the Nature Portfolio Reporting Summary linked to this article.

Data availability

Raw RNA-sequencing data and processed data have been deposited in the NCBI Gene Expression Omnibus (GEO) under accession number GSE165751. MGE clusters identified in Extended Data Fig. 2c are available in Supplementary Table 4. Conservation of *arc* genes performed on metagenomic reads has been deposited under BioProject ID PRJNA748262[28]. Conservation of *arc* genes among enterococci performed on dataset has been deposited under BioProject ID PRJNA587161[25,26]. Source data are provided with this paper.

Code availability

Code and source data for replication of the *C. difficile* GENRE (iCdR703) analyses are available at https://github.com/mjenior/Smith_etal_Enterococcus.

36. Stabler, R. A. et al. Comparative genome and phenotypic analysis of *Clostridium difficile* 027 strains provides insight into the evolution of a hypervirulent bacterium. *Genome Biol.* **10**, R102 (2009).
37. Carter, G. P. et al. Defining the roles of TcdA and TcdB in localized gastrointestinal disease, systemic organ damage, and the host response during *Clostridium difficile* infections. *mBio* **6**, e00551 (2015).
38. Hanahan, D. Studies on transformation of *Escherichia coli* with plasmids. *J. Mol. Biol.* **166**, 557–580 (1983).
39. Dale, J. L. et al. Comprehensive functional analysis of the *Enterococcus faecalis* core genome using an ordered, sequence-defined collection of insertional mutations in strain OG1RF. *mSystems* **3**, e00062–18 (2018).
40. Theriot, C. M. et al. Cefoperazone-treated mice as an experimental platform to assess differential virulence of *Clostridium difficile* strains. *Gut Microbes* **2**, 326–334 (2011).
41. Kumar, L., Cox, C. R. & Sarkar, S. K. Matrix metalloprotease-1 inhibits and disrupts *Enterococcus faecalis* biofilms. *PLoS One* **14**, e0210218 (2019).
42. Bloedt, K., Riecker, M., Poppert, S. & Wellinghausen, N. Evaluation of new selective culture media and a rapid fluorescence in situ hybridization assay for identification of *Clostridium difficile* from stool samples. *J. Med. Microbiol.* **58**, 874–877 (2009).
43. Wellinghausen, N., Bartel, M., Essig, A. & Poppert, S. Rapid identification of clinically relevant *Enterococcus* species by fluorescence in situ hybridization. *J. Clin. Microbiol.* **45**, 3424–3426 (2007).
44. Knippel, R. J. et al. Heme sensing and detoxification by HatRT contributes to pathogenesis during *Clostridium difficile* infection. *PLoS Pathog.* **14**, e1007486 (2018).
45. Dixon, P. VEGAN, a package of R functions for community ecology. *J. Veg. Sci.* **14**, 927–930 (2003).
46. Calle, M. L., Urrea, V., Boulesteix, A. L. & Malats, N. AUC-RF: a new strategy for genomic profiling with random forest. *Hum. Hered.* **72**, 121–132 (2011).
47. Hankin, J. A., Barkley, R. M. & Murphy, R. C. Sublimation as a method of matrix application for mass spectrometric imaging. *J. Am. Soc. Mass. Spectrom.* **18**, 1646–1652 (2007).
48. Thomas, A., Charbonneau, J. L., Fournaise, E. & Chaurand, P. Sublimation of new matrix candidates for high spatial resolution imaging mass spectrometry of lipids: enhanced information in both positive and negative polarities after 1,5-diaminonapthalene deposition. *Anal. Chem.* **84**, 2048–2054 (2012).
49. Yang, J. & Caprioli, R. M. Matrix sublimation/recrystallization for imaging proteins by mass spectrometry at high spatial resolution. *Anal. Chem.* **83**, 5728–5734 (2011).
50. Prentice, B. M. et al. Dynamic range expansion by gas-phase ion fractionation and enrichment for imaging mass spectrometry. *Anal. Chem.* **92**, 13092–13100 (2020).
51. Schneider, C. A., Rasband, W. S. & Eliceiri, K. W. NIH Image to ImageJ: 25 years of image analysis. *Nat. Methods* **9**, 671–675 (2012).
52. Jackson, S., Calos, M., Myers, A. & Self, W. T. Analysis of proline reduction in the nosocomial pathogen *Clostridium difficile*. *J. Bacteriol.* **188**, 8487–8495 (2006).
53. Evans, D. R. et al. Systematic detection of horizontal gene transfer across genera among multidrug-resistant bacteria in a single hospital. *eLife* **9**, e53886 (2020).
54. Seemann, T. Prokka: rapid prokaryotic genome annotation. *Bioinformatics* **30**, 2068–2069 (2014).
55. Shannon, P. et al. Cytoscape: a software environment for integrated models of biomolecular interaction networks. *Genome Res.* **13**, 2498–2504 (2003).
56. Bryan, E. M., Bae, T., Kleerebezem, M. & Dunny, G. M. Improved vectors for nisin-controlled expression in Gram-positive bacteria. *Plasmid* **44**, 183–190 (2000).
57. Chilambi, G. S. et al. Evolution of vancomycin-resistant *Enterococcus faecium* during colonization and infection in immunocompromised pediatric patients. *Proc. Natl Acad. Sci. USA* **117**, 11703–11714 (2020).
58. Page, A. J. et al. Roary: rapid large-scale prokaryote pan genome analysis. *Bioinformatics* **31**, 3691–3693 (2015).
59. Obeid, J. S. et al. Procurement of shared data instruments for Research Electronic Data Capture (REDCap). *J. Biomed. Inform.* **46**, 259–265 (2013).

Acknowledgements We thank L. Harrison and J. Marsh for sharing genome sequence data and VRE isolates from the EDS-HAT study (R01AI127472); the Children's Hospital of Philadelphia Junior Faculty Breakfast Club and the Children's Hospital of Philadelphia MICRO group for feedback on the manuscript; all members of the Zackular laboratory for providing feedback and support; the Children's Hospital of Philadelphia Biostatistics and Data Management Core for statistical consulting and support; E. Friedman and the Penn Microbial Culture and

Metabolomics Core for their support and expertise; and K. Bittinger and C. Tanes for thoughtful discussions on analyses detailed in this study. Funding was provided by the National Institutes of Health grant K22AI7220 (J.P.Z.), National Institutes of Health grant R35GM138369 (J.P.Z.), Children's Hospital of Philadelphia Junior Faculty Pilot Grant (J.P.Z.), Cell and Molecular Biology Training Grant T32GM07229 (A.B.S.), National Institutes of Health grant R01AI138581 (E.P.S.), National Institutes of Health grant R01AI145992 (E.P.S.), National Institutes of Health grant R01AI164587 (E.P.S.), UVA TransUniversity Microbiome Initiative Pilot Grant (M.L.J. and J.A.P.), National Institutes of Health grant R01AT010253 (J.A.P.), Chemical and Biology Interface Training Grant 5T32GM071339-15 (K.A.B.), National Institutes of Health grant R01HD090061 (J.A.G.), National Institutes of Health/National Center for Advancing Translational Sciences Grant Support (UL1TR000445) for REDCap (Vanderbilt University) (M.R.N.), National Institutes of Health grant K23AI156132-01 (M.R.N.), National Institutes of Health grant K23 AI121485 (B.J.K.), Centers for Disease Control and Prevention grant BAA 200-2016-91937 (B.J.K.), Perelman School of Medicine/Children's Hospital of Philadelphia PennCHOP Microbiome Program (R.N.B.), Crohn's and Colitis Foundation (R.N.B.), Penn Center for AIDS Research P30-AI045008 (R.N.B.) and Commonwealth Universal Research Enhancement programme grant SAP#4100068710 (R.N.B.)

Author contributions A.B.S., E.P.S. and J.P.Z. conceived the study. A.B.S. and J.P.Z designed and performed experimentation and mouse work with support from O.K. P.C.R., J.L.H., C.L., J.G., M.A.S. and J.A.G. B.M.P. and J.S. performed the imaging mass spectrometry and analyses. K.A.B. and M.L.M. developed the hydrazine probe and performed corresponding analyses. B.J.K., F.D.B., J.E., R.N.B. and M.R.N. provided human samples and related analyses. M.L.J. and J.A.P. developed *C. difficile* genome-scale metabolic network reconstructions. A.A. and C.D. supported data analyses and bioinformatics. E.E.F. performed pathology analyses. D.R.E. and D.V.T. performed the MGE analyses and collagen-binding assay. Transposon library and biofilm support was provided by G.M.D. Funding was acquired by E.P.S., B.M.P., M.L.J., M.L.M., J.A.P., J.A.G., M.R.N., B.J.K., A.B.S. and J.P.Z. The Article was written by A.B.S. and J.P.Z. with input from the other authors. J.P.Z supervised the research.

Competing interests The authors declare no competing interests.

Additional information

Supplementary information The online version contains supplementary material available at https://doi.org/10.1038/s41586-022-05438-x.

Correspondence and requests for materials should be addressed to Joseph P. Zackular.

Peer review information *Nature* thanks Robert Britton and the other, anonymous, reviewer(s) for their contribution to the peer review of this work.

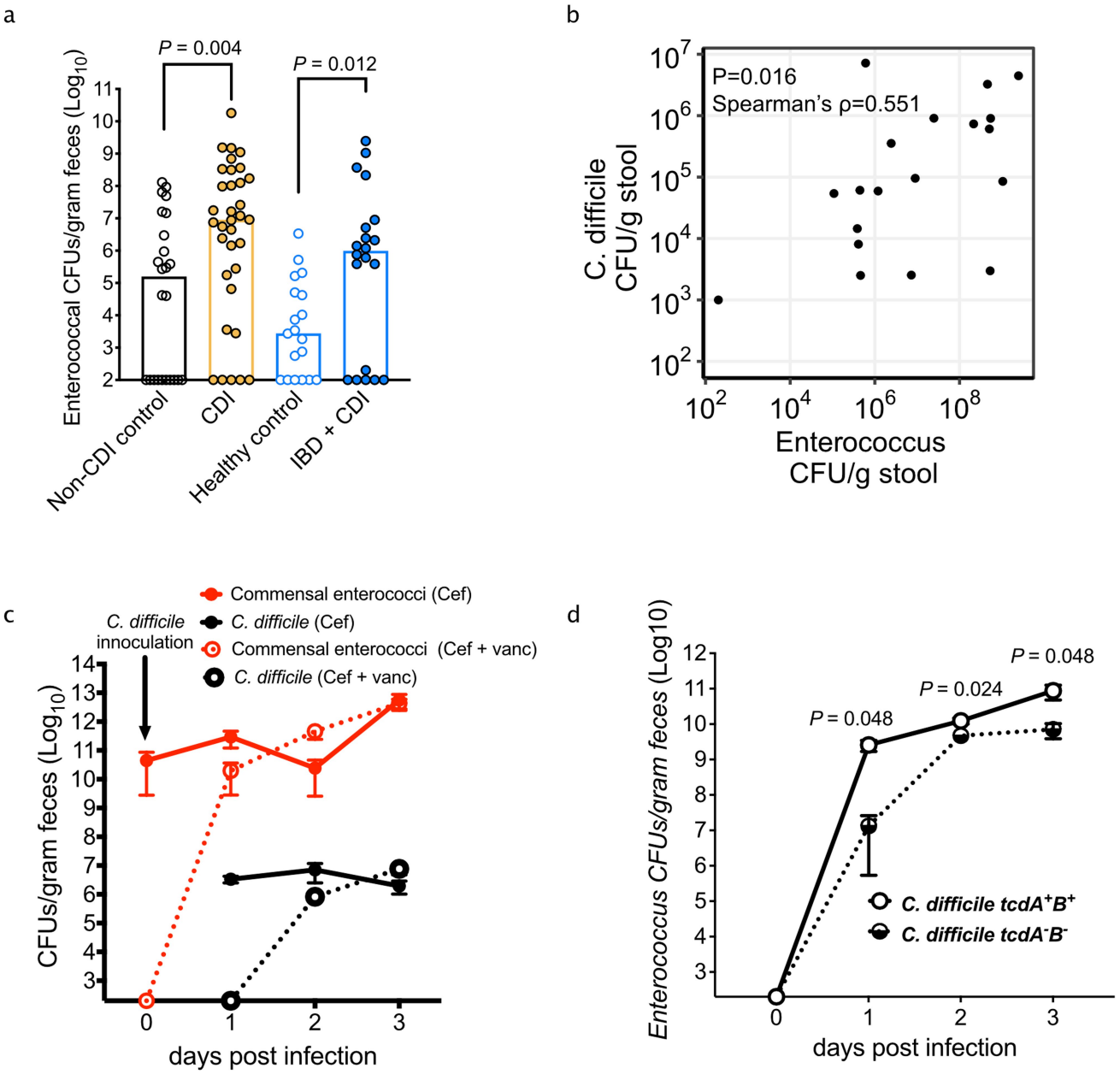

Extended Data Fig. 1 | Enterococcal abundance and dynamics during CDI. (**a**) Enterococcal bacterial burdens (CFUs) from pediatric patients (black and gold = Vanderbilt University (median, n = 24 for Non-CDI controls; n = 34 for CDI, two-sided Mann-Whitney, $P = 0.004$); blue and light blue = Children's Hospital of Philadelphia (n = 19 for healthy; n = 20 for IBD + CDI, two-sided Mann-Whitney test, $P = 0.012$). (**b**) Two-sided Spearman correlation between detected *C. difficile* and *Enterococcus* burdens in pediatric patients with IBD + CDI (Spearman $\rho = 0.551$; n = 19). (**c**) Bacterial burdens quantified from mice following treatment with cefoperazone (cef) or cef + vancomycin (vanc) (mean ± s.e.m., n = 10 mice/group). (**d**) Enterococcal CFUs over the course of CDI. Mice were infected with a toxin producing wild type strain (M7404 TcdA$^+$TcdB$^+$) or a toxin-null isogenic mutant (M7404 TcdA$^-$TcdB$^-$) (n = 5/group) (mean ± s.e.m. two-sided Mann-Whitney with Bonferroni-Dunn method for correction for multiple comparisons, corrected *P* values are in Supplementary Table 5).

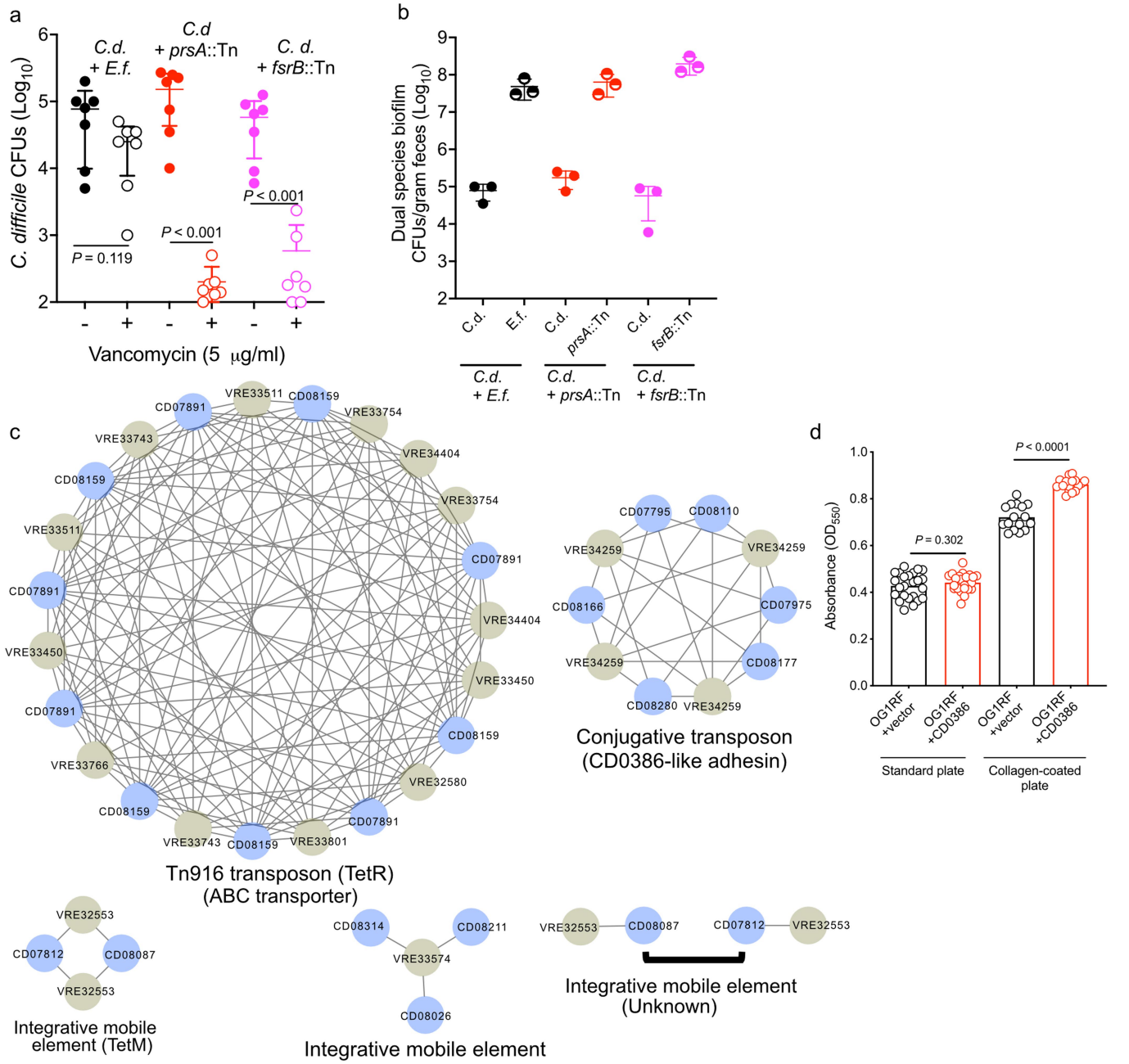

Extended Data Fig. 2 | Biofilm formation and transfer of mobile genetic elements during interspecies interactions. (**a**) Survival assay of co-culture biofilms with *E. faecalis* (*E.f.*) ($P = 0.119$) or transposon mutants in *E. faecalis* genes OG1RF_11528 (*fsrB*::Tn) ($P < 0.001$) and OG1RF_10423 (*prsA*::Tn) ($P < 0.001$). Abundance of *C. difficile* in untreated (-) or vancomycin treated (+) biofilms are depicted (mean ± s.d., n = 7, two-sided Mann-Whitney with Bonferroni-Dunn method for correction for multiple comparisons) (**b**) Abundance of *C. difficile* (*C.d.*) and *E. faecalis* strains (*E.f.*, *prsA*::Tn, and *frsB*::Tn) in untreated dual species biofilms (mean ± s.d., n = 3). (**c**) Clusters of shared sequences detected in *C. difficile* (blue) and VRE (olive) genomes of clinical isolates from hospitalized patients. Lines connect sequences with at least 99.98% identity. Clusters are labeled based on mobile element type and relevant cargo, if known. Source data for each cluster can be found in Supplementary Information. (**d**) Biofilm formation of *E. faecalis* OG1RF carrying empty pMSP3535 vector or pMSP3535 carrying the CD0386-like adhesin. Biofilm formation was tested in standard ($P = 0.302$) and collagen-coated plates ($P<0.001$). Crystal violet staining (OD_{550}) values were calculated (mean ± s.d., n = 24/group for standard plates and 16/group for collagen plates, unpaired two-tailed *t*-tests).

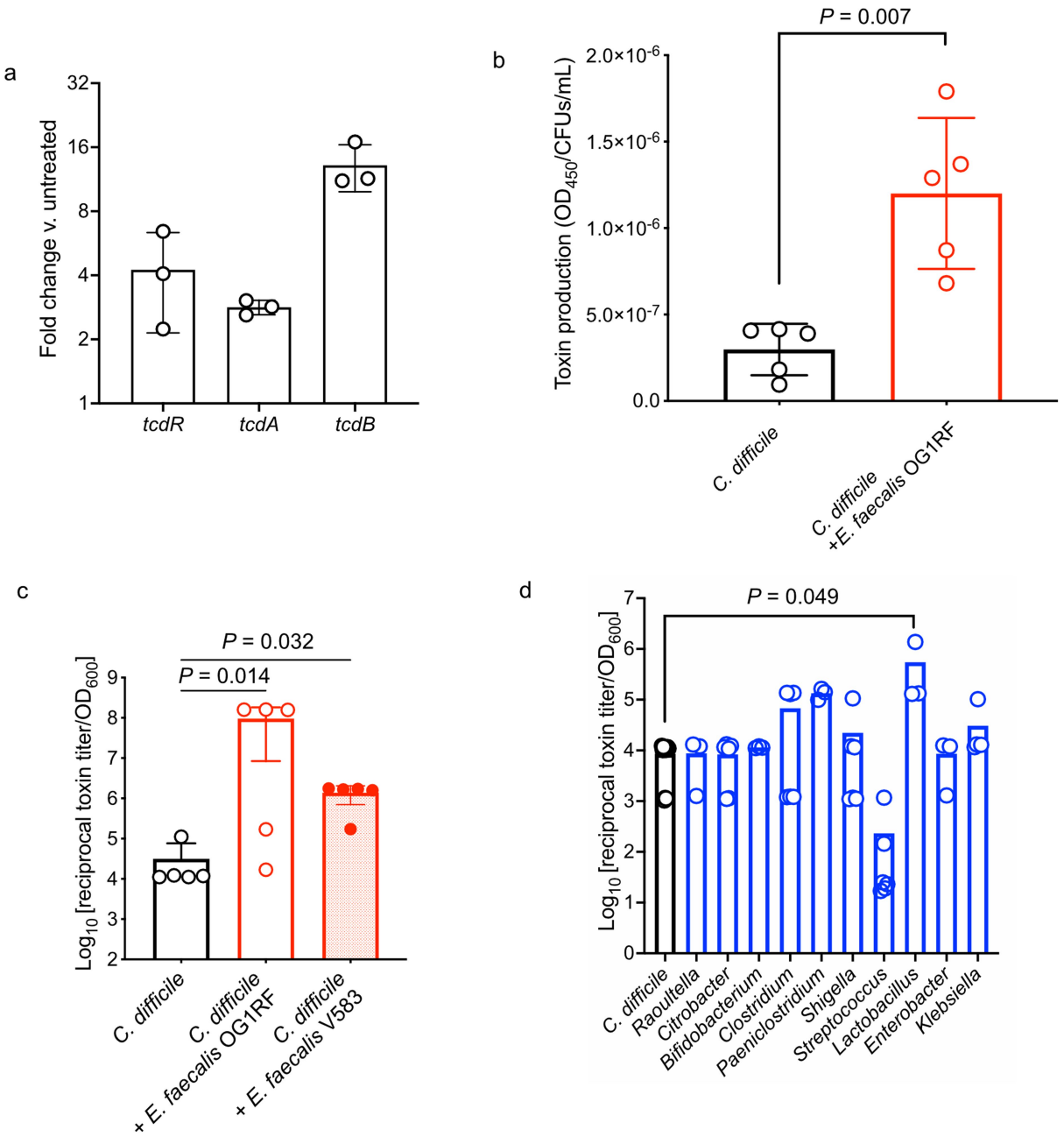

Extended Data Fig. 3 | Enterococcal-mediated enhancement of *C. difficile* toxin gene expression and production. (**a**) Fold change of the toxin-encoding genes in *C. difficile* in coculture with *E. faecalis* versus monoculture as measured by qPCR (mean ± s.d., n = 3). (**b**) Toxin production by *C. difficile* when grown in co-culture with *E. faecalis* as measured by ELISA. Both *C. difficile* and *E. faecalis* were grown in the same culture and differential plating was used to measure *C. difficile* CFUs. Toxin levels (OD_{450}) were normalized to *C. difficile* CFUs in the culture to control for any difference in growth (mean ± s.d., n = 5, two-tailed *t*-tests with Welch's correction, $P = 0.007$). (**c**) *C. difficile* toxin levels measured from *in vitro* cultures by cytotoxicity with *E. faecalis* cell-free supernatants. (mean ± s.d., n = 5, Kruskal-Wallis test with Dunn's correction for multiple comparisons, OG1RF $P = 0.014$, V583 $P = 0.032$). (**d**) *C. difficile* toxin production measured by cytotoxicity following introduction of cell-free supernatants from microbiota isolates cultured from human patients with CDI and IBD (mean ± s.d., n = 12 (*C. difficile*), 3 (*Raoultella, Bifidobacterium, Enterobacter, Paeniclostridium, Lactobacillus*), 5 (*Klebsiella*), 6 (*Citrobacter, Clostridium, Shigella, Streptococcus*), Kruskal-Wallis test with Dunn's correction for multiple comparisons, *Lactobacillus* $P = 0.049$). Isolates were selected to represent the spectrum of taxa cultured from these patients.

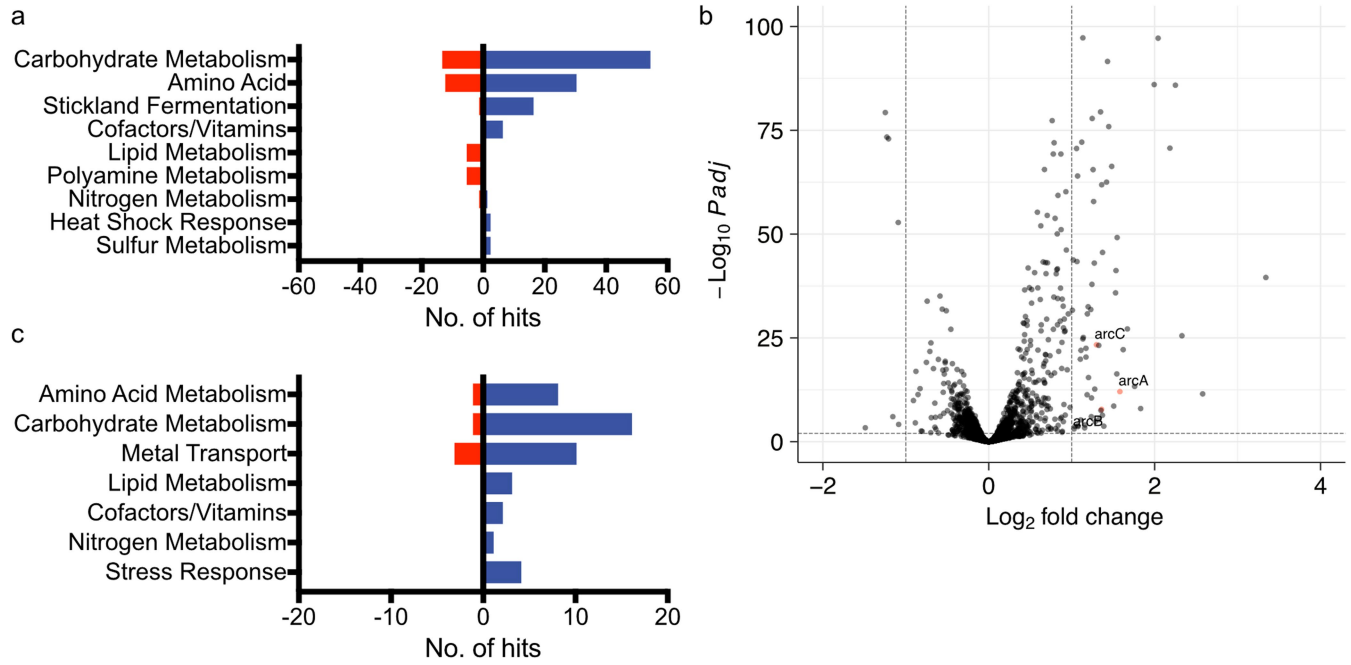

Extended Data Fig. 4 | Transcriptional changes associated with *C. difficile* – *E. faecalis* interactions. (**a**) Pathway analysis of *C. difficile* transcripts significantly altered following co-culture as measured by RNA sequencing. For pathway analyses, blue bars represent transcripts that increased in abundance and red bars represent transcripts that decreased in abundance. (**b**) Volcano plot showing *E. faecalis* transcripts significantly altered following co-culture as measured by RNA sequencing. Red points represent genes associated with amino acid metabolism. Significance determined using two-sided Wald test and corrected for multiple comparisons using the Benjamini-Hochberg method. (**c**) Pathway analysis of *E. faecalis* transcripts significantly altered following co-culture as measured by RNA sequencing.

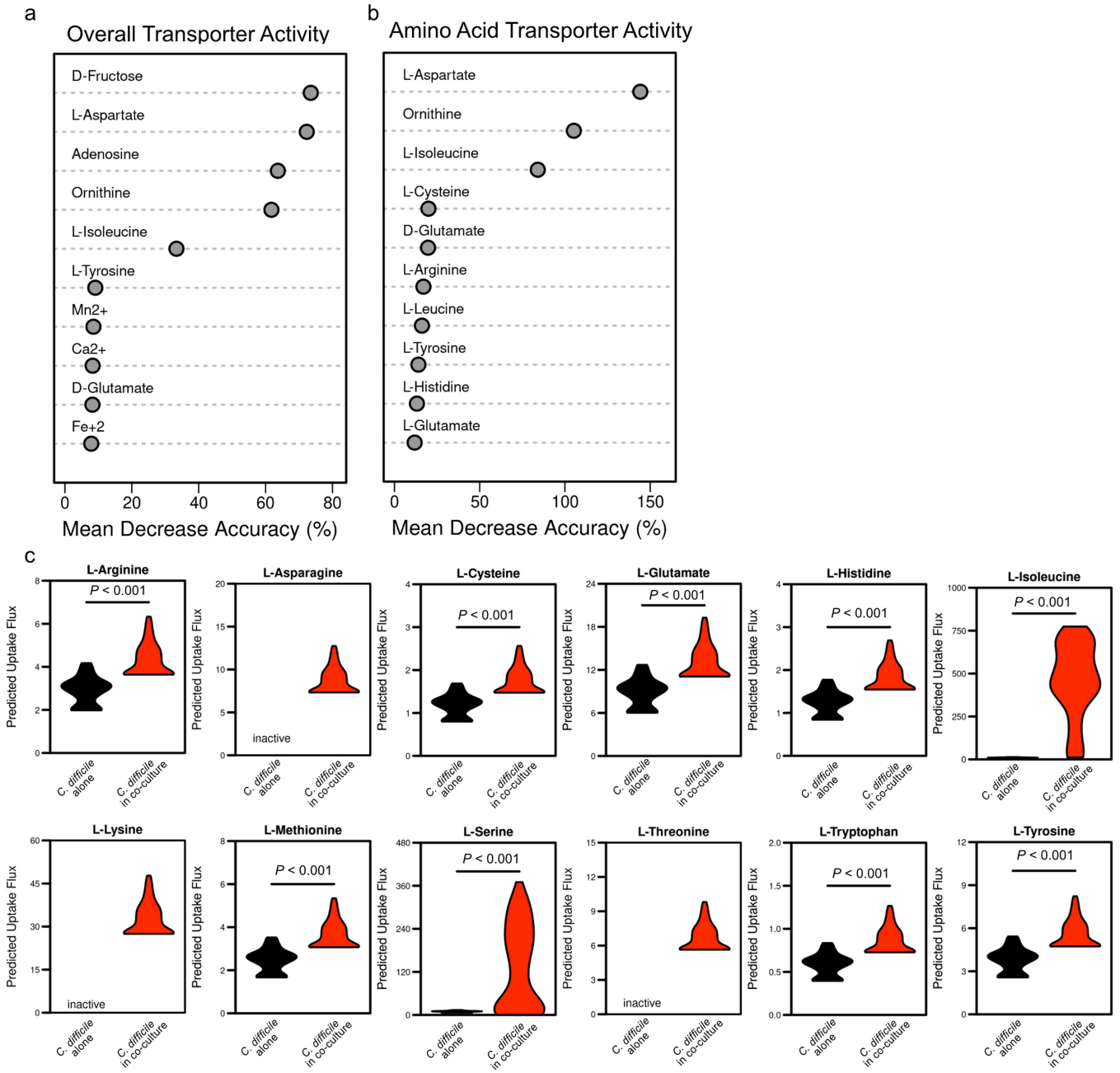

Extended Data Fig. 5 | Transcriptome-guided metabolic flux predictions using genome-scale metabolic network reconstruction for *C. difficile*. (**a**) AUC-Random Forest supervised machine learning results for reaction flux samples for conserved transport reactions between contexts (k = 10; OOB = 0%). (**b**) AUC-Random Forest supervised machine learning results for reaction flux samples for conserved amino acid transport reactions between contexts (k = 10; OOB = 0%). (**c**) Difference in simulated uptake of selected amino acids across context-specific models. Significance determined by two-sided Wilcoxon rank-sum test. Corrected *P* values in Supplementary Table 5.

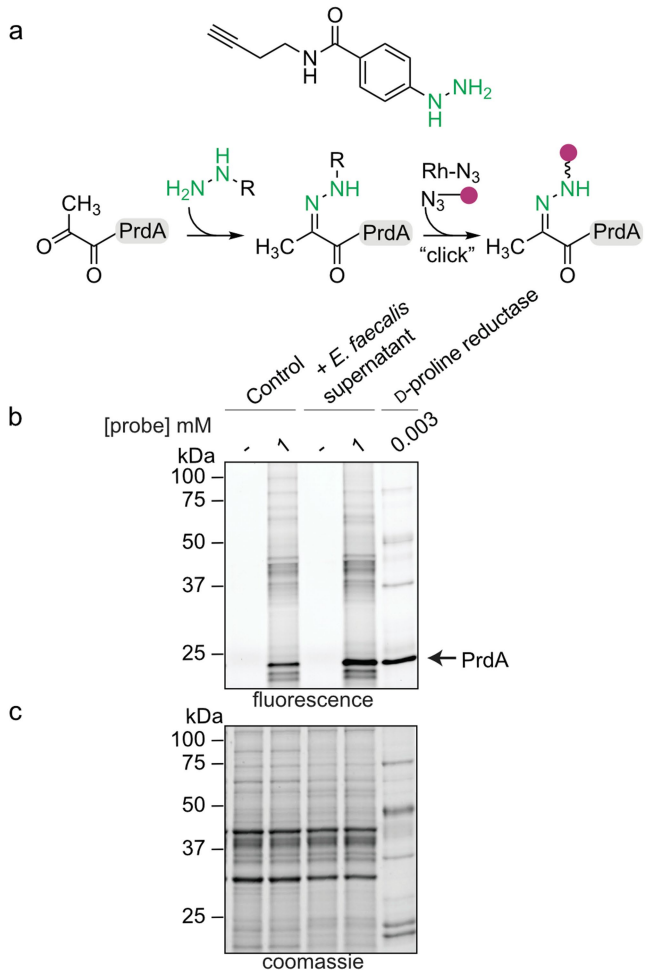

Extended Data Fig. 6 | *In situ* labelling of *C. difficile* with a hydrazine probe and gel-based profiling of D-proline reductase activity. (**a**) Labeling schematic of hydrazine probe with PrdA of D-proline reductase. (**b**) Representative gel-based labelling profiles for *C. difficile* in the absence and presence of *E. faecalis* supernatant. Gel representative of three separate experiments. For Gel source data, see Supplementary Fig. 1. (**c**) Corresponding expression profiles after Coomassie staining.

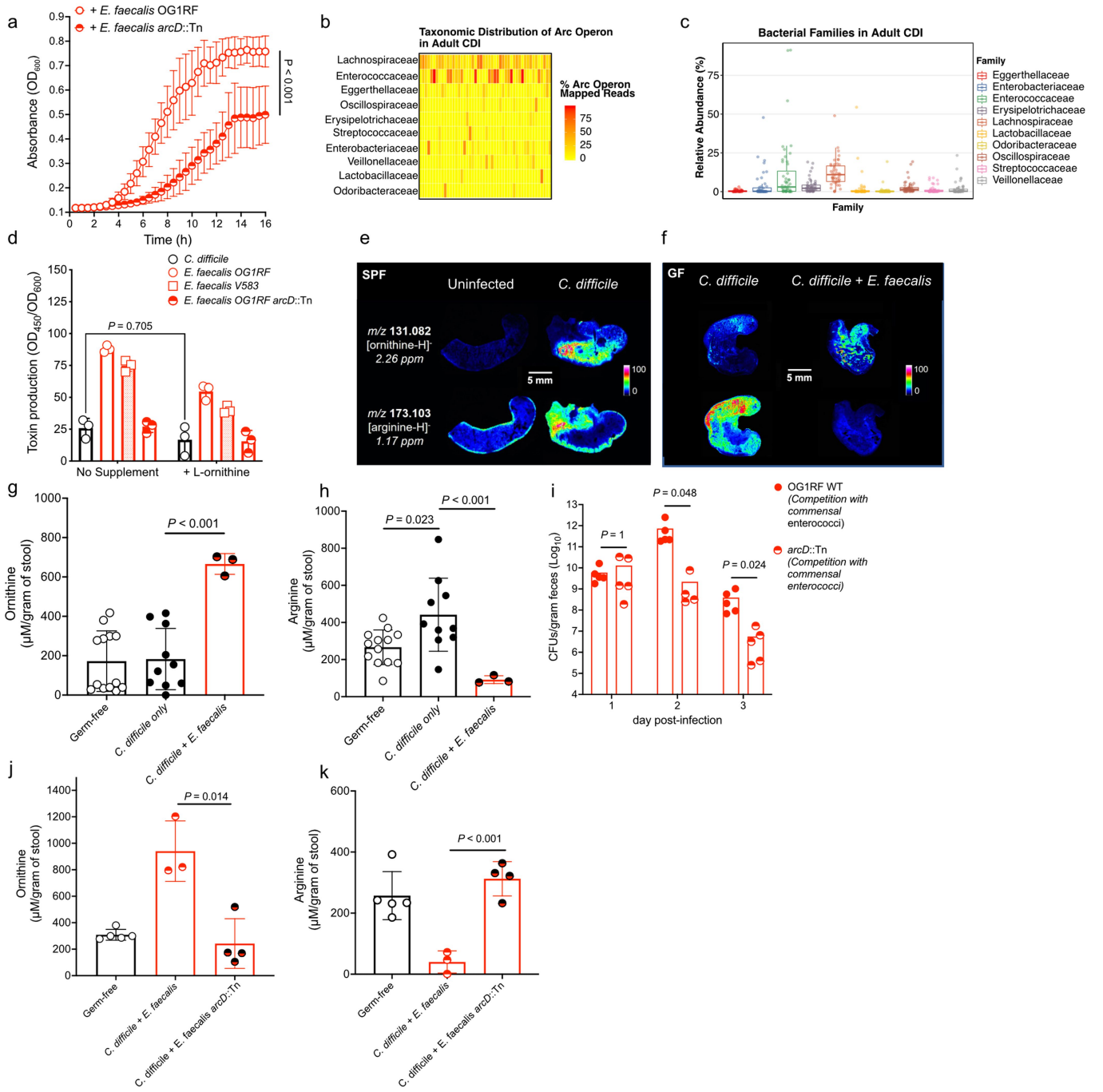

Extended Data Fig. 7 | The enterococcal ADI pathway reshapes the metabolic environment in the gut during CDI. (**a**) *C. difficile* growth in presence of *E. faecalis* or *E. faecalis arcD*::Tn supernatants. (mean ± s.d., n = 8/group, two-way ANOVA, Time factor $P < 0.001$). (**b**) Taxonomic distribution (at bacterial family level) of reads mapped to *arc* genes in adult patients (n = 48) with symptomatic CDI. Each column is a subject and each row is a bacterial family. Each cell displays the percentage of reads mapped to *arc* genes of a specific family out of all *arc* mapped reads. (**c**) Relative abundance of the top 10 *arc* operon containing bacterial families in each adult patient symptomatically infected with *C. difficile* (n = 48, lower and upper hinges correspond to the first (25%) and third (75%) quartiles. The upper and lower whiskers extend from the hinge to the largest value no further than 1.5*IQR. Data beyond the whiskers are plotted individually). (**d**) Toxin production of *C. difficile* following introduction of supernatants from *E. faecalis* and addition of exogenous L-ornithine measured by ELISA (mean ± s.d., n = 3, Tukey's multiple comparisons test, *C. difficile* +/- ornithine $P = 0.705$). (**e**) MALDI-IMS image of uninfected or infected mice (3d post-infection) (SPF) (representative of n = 5 mice) or (**f**) GF mice mono-infected with *C. difficile* CD196 or co-infected with *E. faecalis* OG1RF (2d post-infection) (representative of n = 4 mice). Individual heatmaps of arginine and ornithine. (**g**) Ornithine levels in stool measured by targeted metabolomics in GF mice infected with *C. difficile* only (mean ± s.d., n = 10) or *C. difficile* + *E. faecalis* OG1RF (mean ± s.d., n = 3, two-sided *t*-tests with Welch's correction, $P < 0.001$). Metabolomics were performed on GF mice prior to infection (GF group, n = 13). (**h**) Arginine levels in stool of GF mice infected with *C. difficile* only (mean ± s.d., n = 10, two-sided *t*-test with Welch's correction, $P = 0.023$) or *C. difficile* + *E. faecalis* OG1RF (mean ± s.d., n = 3, two-sided *t*-test with Welch's correction, $P < 0.001$). Stool metabolomics performed prior to infection (GF group, n = 13). (**i**) CFU of *E. faecalis* OG1RF (wild type) or *E. faecalis arcD*::Tn during CDI. Each strain introduced prior to CDI and naturally competed with endogenous enterococci (n = 5/group) (mean ± s.e.m. two-sided Mann-Whitney test with Bonferroni-Dunn method for correction for multiple comparisons, day 2 $P = 0.048$, day 3 $P = 0.024$). (**j**) Ornithine ($P = 0.014$) and (**k**) arginine ($P < 0.001$) levels in stool measured by targeted metabolomics in GF mice infected with *C. difficile*. Mice pre-colonized for 1 day with *E. faecalis* (n = 3) or *E. faecalis* arcD::Tn (n = 4) (mean ± s.d., two-sided *t*-tests with Welch's correction). Metabolomics performed on GF mice prior to infection (GF group, n = 5).

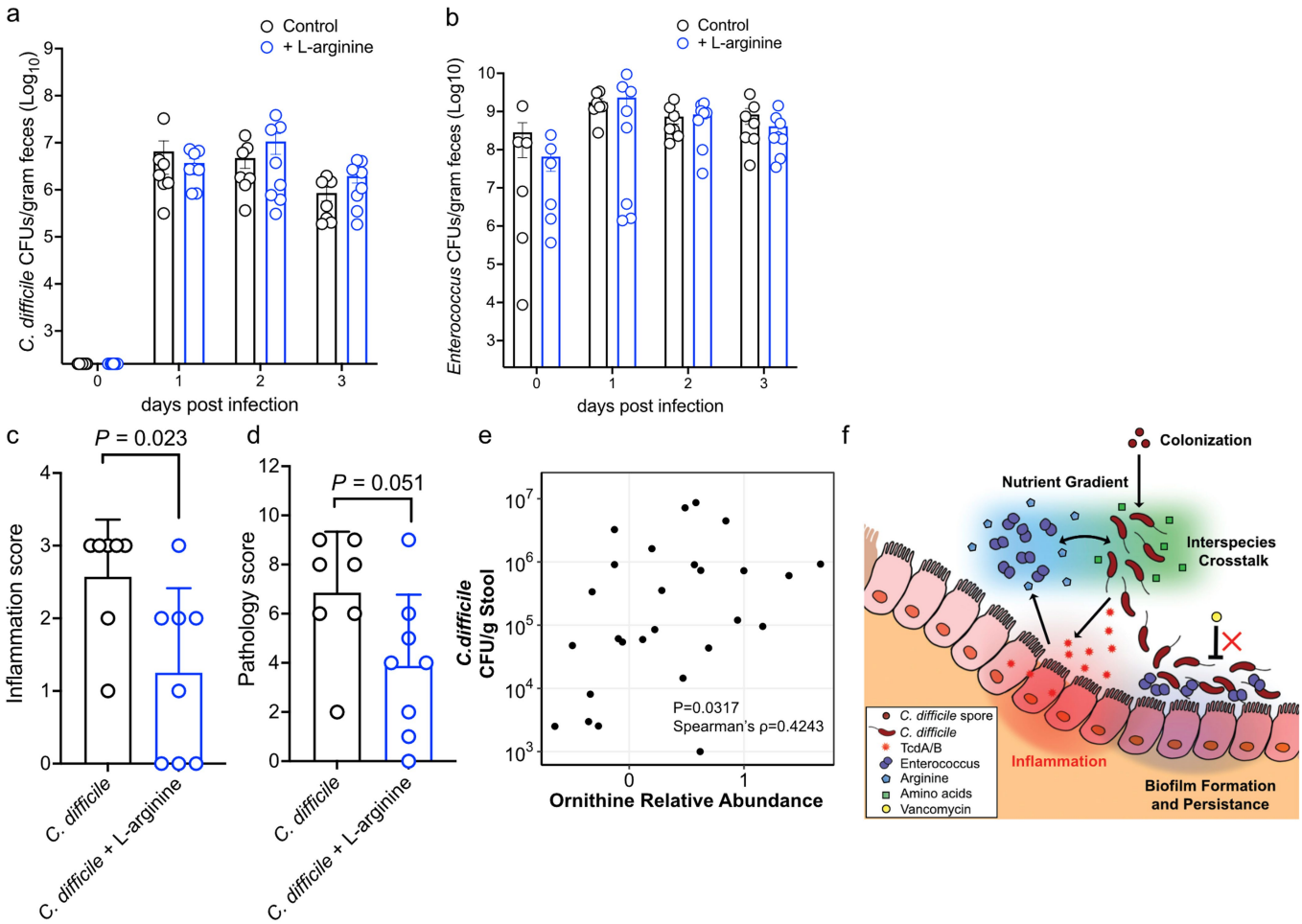

Extended Data Fig. 8 | Arginine supplementation decreases *C. difficile* pathogenesis in mice. (**a**) *C. difficile* and (**b**) *Enterococcus* burdens quantified from mice following cefoperazone treatment and subsequent infection. Mice were treated with 2% L-arginine in drinking water starting 2 days prior to infection and subsequently during the course of infection (mean ± s.d., n = 7 for control, n = 8 for L-arginine treated; Mann-Whitney with Bonferroni-Dunn method for correction for multiple comparisons for each comparison). (**c**) Inflammation score ($P = 0.023$) and (**d**) cumulative pathology score ($P = 0.051$) measured 3 days post-infection for control (n = 7) and L-arginine treated (n = 8) mice (mean ± s.d., two-sided *t*-tests with Welch's correction). (**e**) Spearman correlation between ornithine abundance in stool and *C. difficile* burdens in pediatric patients with IBD and CDI with detectable *C. difficile* based on culture (two-sided Spearman's $\rho = 0.4243$; n = 26). (**f**) Proposed model of multifaceted cooperative interactions between enterococci and *C. difficile* during infection.

nature research

Corresponding author(s): Joseph P. Zackular

Last updated by author(s): September 18, 2022

Reporting Summary

Nature Research wishes to improve the reproducibility of the work that we publish. This form provides structure for consistency and transparency in reporting. For further information on Nature Research policies, see our Editorial Policies and the Editorial Policy Checklist.

Statistics

For all statistical analyses, confirm that the following items are present in the figure legend, table legend, main text, or Methods section.

n/a	Confirmed	
☐	☒	The exact sample size (*n*) for each experimental group/condition, given as a discrete number and unit of measurement
☐	☒	A statement on whether measurements were taken from distinct samples or whether the same sample was measured repeatedly
☐	☒	The statistical test(s) used AND whether they are one- or two-sided *Only common tests should be described solely by name; describe more complex techniques in the Methods section.*
☐	☒	A description of all covariates tested
☐	☒	A description of any assumptions or corrections, such as tests of normality and adjustment for multiple comparisons
☐	☒	A full description of the statistical parameters including central tendency (e.g. means) or other basic estimates (e.g. regression coefficient) AND variation (e.g. standard deviation) or associated estimates of uncertainty (e.g. confidence intervals)
☐	☒	For null hypothesis testing, the test statistic (e.g. *F*, *t*, *r*) with confidence intervals, effect sizes, degrees of freedom and *P* value noted *Give P values as exact values whenever suitable.*
☒	☐	For Bayesian analysis, information on the choice of priors and Markov chain Monte Carlo settings
☒	☐	For hierarchical and complex designs, identification of the appropriate level for tests and full reporting of outcomes
☒	☐	Estimates of effect sizes (e.g. Cohen's *d*, Pearson's *r*), indicating how they were calculated

Our web collection on statistics for biologists contains articles on many of the points above.

Software and code

Policy information about availability of computer code

Data collection	RNAseq: Processing RNA-Seq ReadsSingle-end RNA-seq reads were trimmed of any adaptor sequences with trim-galore (version 0.6.6). The remaining reads were aligned to the Clostridioides difficile r20291 reference genomeusing STAR (version 2.7.6a) with the following parameters: --outSAMtype BAM SortedByCoordinate --limitBAMsortRAM 1500000000 --outSAMmapqUnique 255 --outFilterMultimapNmax 1 --alignIntronMax 1. Reads count on each gene was calculated at the same time of mapping with the parameter --quantMode GeneCounts. Differential expression analysis between Coculture vs C.difficile alone was done using R package DESeq2 (version 1.30.0). The read counts were normalized among the samples and were transformed to log2 form using the variance stabilizing transformations (VST) method. Volcano plot was drawn using the R package EnhancedVolcano (version 1.8.0). Only the differentially expressed genes (adjusted p-value < 0.01 and fold-change >= 2) were shown on the plot, AA metabolism associated genes were colored in red and only the genes with classic nomenclatures were labeled. 16S rRNA gene sequencing: We extracted DNA from residual stool using the Powersoil kit (Qiagen), amplified the V1-V2 hypervariable region of the 16S rRNA gene using barcoded 27F and 338R primers, and performed paired-end 250bp sequencing (Illumina MiSeq). Sequences were demultiplexed and aligned with QIIME2; sequence denoising and amplicon sequence-variant (ASV) binning was performed with DADA2. Taxonomic assignment was performed by basic local alignment (BLAST) to the SILVA rRNA gene database (version 132).
Data analysis	Code for C. difficile GENRE (iCdR703) analyses are available at https://github.com/mjenior/Smith_etal_Enterococcus.

For manuscripts utilizing custom algorithms or software that are central to the research but not yet described in published literature, software must be made available to editors and reviewers. We strongly encourage code deposition in a community repository (e.g. GitHub). See the Nature Research guidelines for submitting code & software for further information.

Data

Policy information about availability of data

All manuscripts must include a data availability statement. This statement should provide the following information, where applicable:

- Accession codes, unique identifiers, or web links for publicly available datasets
- A list of figures that have associated raw data
- A description of any restrictions on data availability

Raw RNA sequencing data and processed data are deposited in the NCBI Gene Expression Omnibus (GEO) under accession number SE165751. All other data are available in the main text, supplementary materials, or upon publication. No data is restricted.

Field-specific reporting

Please select the one below that is the best fit for your research. If you are not sure, read the appropriate sections before making your selection.

☒ Life sciences ☐ Behavioural & social sciences ☐ Ecological, evolutionary & environmental sciences

For a reference copy of the document with all sections, see nature.com/documents/nr-reporting-summary-flat.pdf

Life sciences study design

All studies must disclose on these points even when the disclosure is negative.

Sample size	Power analyses were not performed prior animal work. Sample sizes were selected based on published and preliminary experimentation (PMCIDs: PMC5101143, PMC6697607, PMC7067591, PMC6325247). For germ-free animal experiments a sample size of five per group was used based on availability of germ-free mice from litters and controlled for age. For conventional mouse work, sample sizes of at least five were used to quantify bacterial burdens longitudinally and sample sizes of >10 per group were used when assaying for initial C. difficile colonization levels or toxin titers.
Data exclusions	No data was excluded. When animals were too sick to form stool due to C. difficile-associated disease, stool-related data is absent.
Replication	All experimental data were replicated at least 3 independent times.
Randomization	Conventional mice were ordered from Jackson laboratories and assigned a treatment group at random. Bedding swaps were performed to normalize for initial microbiota. For germ-free mice, mice were randomly assigned treatment groups.
Blinding	Researchers were unblinded during sample collection in animals due to the importance of controlling for cross contamination of C. difficile spores across groups. For example, uninfected controls were always handled prior to handling of infected mice. Researchers were blinded to treatment groups when quantifying pathological scores.

Reporting for specific materials, systems and methods

We require information from authors about some types of materials, experimental systems and methods used in many studies. Here, indicate whether each material, system or method listed is relevant to your study. If you are not sure if a list item applies to your research, read the appropriate section before selecting a response.

Materials & experimental systems

n/a	Involved in the study
☒	☐ Antibodies
☐	☒ Eukaryotic cell lines
☒	☐ Palaeontology and archaeology
☐	☒ Animals and other organisms
☐	☒ Human research participants
☒	☐ Clinical data
☒	☐ Dual use research of concern

Methods

n/a	Involved in the study
☒	☐ ChIP-seq
☒	☐ Flow cytometry
☒	☐ MRI-based neuroimaging

Eukaryotic cell lines

Policy information about cell lines

Cell line source(s)	Vero cells (ATCC #CCL-81)
Authentication	Cell lines used were not authenticated

Mycoplasma contamination	Cell lines used were not tested for mycoplasma contamination
Commonly misidentified lines (See ICLAC register)	Commonly misidentified cell lines were not used

Animals and other organisms

Policy information about studies involving animals; ARRIVE guidelines recommended for reporting animal research

Laboratory animals	Male C57BL/6 mice ages 6 weeks - 10 weeks were used in this study for conventional animals. Female C57BL/6 mice ages 6 weeks - 10 were used for germ-free and gnotobiotic mice. All mice were housed in micro-isolator cages, housed on individually-ventilated cage racks . Mice were housed at 70-72°F and >30-50% humidity. Mice were given water and food ad libitum and maintained under a 12 hour light cycle.
Wild animals	The study did not involved wild animals
Field-collected samples	The study did not collect field samples
Ethics oversight	All animal research was approved by the IACUC at the Children's Hospital of Philadelphia, University of Pennsylvania, or Vanderbilt University Medical Center

Note that full information on the approval of the study protocol must also be provided in the manuscript.

Human research participants

Policy information about studies involving human research participants

Population characteristics	Vanderbilt University Medical Center: Pediatric participants, ages 12 months through 18 years, were prospectively enrolled from July 2017 through December 2019 at Monroe Carell Jr. Children's Hospital at Vanderbilt after informed parental consent and patient assent when applicable (IRB #170067). Median age (IQR)- 13 years (5-16). Sex distribution was 50% male and 50% female. Children's Hospital of Philadelphia: Subjects were recruited at the Children's Hospital of Philadelphia (CHOP) from September 2015 to April 2018 (IRB approval number 15-011817), as previously described. Age in years (mean (SD)): 11.78 (4.78) for healthy and 12.63 (4.66) for IBD + CDI. Female (%) 26 (68.4) for healthy and 8 (34.8) for IBD+ CDI. The Hospital of the University of Pennsylvania: adult patients were identified over six months of continuous screening (February – August 2017) at the Hospital of the University of Pennsylvania, with a waiver of informed consent granted by the University of Pennsylvania Institutional Review Board (IRB #826543). Sex distribution was 46% male and 54% female.
Recruitment	Vanderbilt University Medical Center: Pediatric participants, ages 12 months through 18 years, were prospectively enrolled from July 2017 through December 2019 at Monroe Carell Jr. Children's Hospital at Vanderbilt after informed parental consent and patient assent when applicable. This study was approved by the Vanderbilt Institutional Review Board (IRB# 170067). Pediatric patients who had positive testing for C. difficile were identified through the clinical lab. The clinical lab at Vanderbilt University Medical Center receives specimens from all inpatient and outpatient encounters. After informed parental consent, residual stool samples were obtained through the clinical lab and transferred to the research laboratory where they were stored at -80 until analysis. Children's Hospital of Philadelphia: Subjects were recruited at the Children's Hospital of Philadelphia (CHOP) from September 2015 to April 2018 (IRB approval number 15-011817), as previously described. Groups included healthy children (HC) and children with IBD and concurrent CDI (IBD+CDI). Healthy children were age matched to those with IBD + CDI. For inclusion in the C. difficile infected group, patients needed to 1) have an underlying diagnosis of inflammatory bowel disease 2) have loose, watery stools at least 3 times per day for >24 hours or an increase in stool frequency from baseline and 3) be positive by glutamate dehydrogenase (GDH) testing assay or PCR for the presence of the toxin A/B gene (cycle of threshold <40). Clinical manifestations of C. difficile infection ranged from mild diarrhea to fulminant colitis and shock. Patients with CDI were identified by notification of positive testing for toxigenic C. difficile by the CHOP Microbiology laboratory. Exclusion criteria included history of hemophagocytic lymphohistiocytosis or Langerhan's cell histiocytosis or concurrent gastrointestinal infection proven by clinical testing. Prior history of C. difficile or recent antibiotic use were not exclusion criteria. Inclusion criteria for healthy controls included if they did not have a chronic diagnosis and could provide stool samples at all 3 time points. Healthy children were excluded if they had diarrhea, antibiotic use in 90 days prior to enrollment, or a family member with C. difficile enrolled into the study. The Hospital of the University of Pennsylvania: Subjects with positive testing by enzyme immunoassay (EIA) for C. difficile toxin A or B were identified over six months of continuous screening (February – August 2017) at the Hospital of the University of Pennsylvania, with a waiver of informed consent granted by the University of Pennsylvania Institutional Review Board (IRB #826543). Fecal specimens from 50 consecutive toxin EIA+ subjects underwent 16S rRNA gene sequencing as described above, and the fecal bacterial community composition was compared to the maximum peripheral white blood cell (WBC) count within 72 hours of the index C. difficile test. WBC data were extracted from the subjects' electronic medical records. All adult patients were asked if they were willing to participate in these studies and a waiver of informed consent granted by each aforementioned Institutional Review Board.
Ethics oversight	The IRB at the Vanderbilt University Medical Center, Children's Hospital of Philadelphia, or the Hospital of the University of Pennsylvania approved all included human studies

Note that full information on the approval of the study protocol must also be provided in the manuscript.